Variations in Material Properties of Grey Cast Iron and its Impact on Tool Wear

Andreas Söderholm

2021

CODEN:LUTMDN/(TMMV-5309)1-102/2021

MASTER THESIS
DIVISION OF PRODUCTION AND MATERIALS ENGINEERING
LUND UNIVERSITY

Supervisor:
Christina Windmark, PhD, Production and Materials Engineering, Lund University

Co Supervisor:
Rebecka Lindvall, Doctoral student, Production and Materials Engineering, Lund University

Industrial Supervisor:
Sebastian Sirén, Manufacturing Technology Specialist, Volvo Trucks Operations

Examiner:
Jan-Eric Ståhl, Professor, Production and Materials Engineering, Lund University

Author: Andreas Söderholm
Lund, Sweden 2021

Avdelningen för Industriell Produktion
Lunds Tekniska Högskola
Lunds universitet
Box 118
221 00 Lund
Sverige

Division of Production and Materials Engineering
LTH, School of Engineering
Lund University
Box 118
SE-221 00 Lund
Sweden

Printed in Sweden
Media-Tryck
Lund University

Preface

This master thesis is enabled trough the Vinnova project *Sustainable production realization of cast iron components in an extended value chain, dnr: 2019-03118* with the purpose of accumulate knowledge about the behavior of grey cast iron during machining when the proportion of recycled material in casted parts is increased.

The master thesis was performed in collaboration with the Volvo Group Trucks Corporation and the Division of Production and Materials Engineering, Department of Mechanical Engineering, Faculty of Engineering at Lund University and carried out during the time period of 7th September 2020 to 12th February 2021 at the Volvo Trucks plant in Skövde, Sweden.

Both practical and theoretical work was carried out in order to write this thesis. Collection of material and cutting tool samples and analyzes of these were done as well as theoretical studies of the subject.

I would like to thank my examiner, Jan-Eric Ståhl, who got me the opportunity to write my master thesis at such a large and respected Swedish corporation as AB Volvo, and whose charisma and knowledge about industrial production was the reason I chose to study at the Division of Production and Materials engineering in the first place.

I also owe great gratitude to my supervisor Christina Windmark, whose helpfulness, professionalism and expertise about academic writing got me through the master thesis process, and to my co-supervisor Rebecka Lindvall whose positive attitude and understanding of the student's point of view was equally important in finishing the thesis.

My industrial supervisor, Sebastian Sirén, thank you for the time and effort you gave me. I fully appreciated the knowledge about the subject you have, and all the guidance, patience and help I got from you.

Last, but not least, I would like to deeply and sincerely thank my parents Göran and Agneta Söderholm and my sister Rebecka Lyhne for believing in me and supporting me through my whole student time, without you none of this would have been possible. Now I am finally an engineer!

Lund 2021-02-12

Andreas Söderholm

"Ask of the Steel, each Strut and Wire,
Ask of the Searching, Purging Fire,
That Marked their Natal Hour,
Ask of the Mind, the Hand, the Heart,
Ask of each Single, Stalwart Part,
What Gave it Force and Power."

- The Mighty Task is Done,
Joseph B. Strauss, 1937

Abstract

Among cast materials, grey cast iron and ductile iron makes up about three quarters of all cast parts. This makes the manufacturing and machining of grey cast iron an important economical factor for the automotive industry.

In a world with finite resources and growing concerns for the environment the importance and interest in recycling grows larger. This has led the Volvo Trucks Corporation to use a higher quantity of recycled metal in their casted parts. The increase in recycled metal causes an increase in the quantity of impurities and trace elements, which could potentially lower the machinability of the grey cast iron used in the engine blocks of Volvo trucks.

Currently, the Volvo Trucks Corporation experience a high unpredictability of the tool wear when machining engine blocks, this study investigates how the properties of the workpiece material differs between manufactured series of engine blocks and how this impacts the degree of tool wear. This was done by collecting and examining of cutting tools from a rough milling operation in one of Volvos production lines as well as examining material samples from engine blocks machined by said cutting tools.

The evaluated workpiece material properties were the chemical content, the graphite structure, the hardness, and the concentration of hard inclusions. The material properties were put in relation to the degree of tool wear.

The results shows that there was considerable variations in the degree of tool wear between the studied series, ranging from virtually undamaged to severe fractures. Severe degree of tool wear had a strong correlation with a high concentration of inclusions. The concentration of inclusions were in turn higher in samples with a high content of trace elements. The result also shows that a large number of material samples had an undesired graphite distribution of type D and E instead of type A. The hardness of the workpiece material was fairly consistent in all samples but showed a weak correlation between high hardness and graphite distribution of type E or D. Harder materials were in general easier to machine, which probably can be explained by a lower concentration of inclusions.

Keywords: Grey cast iron, Hard inclusions, Tool wear, Machinability, Graphite structure.

Table of Content

1. Introduction

The automotive industry is today one of the largest users of cast materials. Within this material group, three quarters of the casted parts are made of grey cast iron or ductile iron. There are many reasons for the popularity of grey cast iron, including desirable properties like good wear resistance, high hardness, and ease of production and machinability that leads to low costs [1].

Even though grey cast iron is one of the most used materials in the industry and it has been around in various forms for more than hundred years, its behavior during machining and the impact of factors such as quantity of trace elements, aging time or cooling time are not yet fully understood [1].

In recent years, the unending demand for lowering costs in the automotive industry and the growing concerns in society for the environment has led to an increase in the amount of recycled metal used in the casting industry. The use of recycled metal will inevitably lead to an increase in unwanted impurities and other trace elements that will affect the workpiece material in unpredictable ways.

Currently, the Volvo plant in Skövde experience a high and unpredictable variation of the cutting tool wear when machining casted engine blocks. Unpredictable tool wear has led to a more conservative number of parts being machined by the cutting tools before replacement to avoid premature tool failure. With short intervals of tool replacements comes an increased cost of tools and downtimes due to tool handling.

The wear on the cutting tools are classified and statistically analyzed. By also examining the workpiece material from a number of different aspects and comparing this to the wear pattern on the cutting tools, a deeper understanding of what causes the variation of tool wear will be obtained. Properties of the workpiece material that are analyzed are the graphite structure, the chemical content, the hardness and the concentration and composition of the inclusions.

1.1. Problem description

How the degree of tool wear varies between machined series of engine blocks, and what impact the workpiece material properties of the grey cast iron have on this variation of tool wear.

1.2. Purpose

The purpose of this study is to further accumulate knowledge of material properties of grey cast iron and its impact on tool wear and machinability.

Knowledge about the material properties and its consequences is crucial for selecting the optimal cutting tools and cutting data and can be used to predict the tool wear, thus enable optimal use of cutting tools and avoidance of rapid cutting edge failure.

1.3. Scope

This report will focus on the material properties hardness, graphite structure and titanium carbonitrides Ti(C,N). The chemical composition of the workpiece material grey cast iron will only be related to these factors. The tool wear will be classified in terms of type and severeness, and linked to the material properties described.

1.4. Limitations

This report will not suggest any counter measures to the excessive tool wear that occasionally occurs in the machining of grey cast iron. That is, only the cause, and not the solution, of the problem will studied. Furthermore, the impact of other types of inclusions than Ti(C,N) on the tool wear or other material factors than hardness and graphite structure will not be a part of this report. The study of tool wear will be limited to the rough milling operation, at the workstation OP20 at the 11-liters engine block manufacturing line at the Volvo Truck plant in Skövde, Sweden.

2. Theory

In this chapter the theories of which this study is based is presented. It includes background information about the material properties of grey cast iron as well as theories about how alloying elements affects it. The concept of machinability and common types of cutting tool wear are explained. Theories about how hard inclusions in grey cast iron affects the material and the machinability are also presented. Lastly, the functioning and purpose of a Scanning Electron Microscope and a Brinell hardness test are explained.

2.1. Grey cast iron

Grey cast iron is, as the name implies, a member of the material group cast ferrous alloys. It is by far the most common alloy in this material group, in 2018 grey cast iron constituted 43% of the world's total production of casted metals [2].

Casting is a very common and old method to produce metallic parts and it gains its popularity from its simplicity. It is produced by letting molten metal pour into a cavity of desired shape, this leads to a geometry that is very close to the final form of the part that is to be manufactured. Casted parts are widely used in the automotive industry where they are used for their functionality and low manufacturing costs. Typical parts that are made of grey iron are cylinder heads and blocks, flywheels and brake discs [3].

Grey iron has a good machinability in relation to many other materials and is comparable to steel in this aspect [3]. The chips that are produced during machining are discontinuous and the chip control is rarely a problem. What limits the machinability is often the presence of so called white iron. White iron is a variant of grey iron which is very hard and results in a high level of abrasive wear and is formed when the cooling is too rapid, which is often the case in thin sections of a part or at its corners. To reduce the formation of white iron this should be taken into account when designing the castings, thus overly complex geometries should be avoided when using grey cast iron. A wide variety of cutting tool materials can be used to machine grey iron, for example cemented carbides, ceramics and polycrystalline cubic boron nitride (pcBN) [1].

The alloying elements used in grey iron does not automatically determine its mechanical characteristics. Other factors such as the microstructure, the level of impurities it contains, the cooling rate and the dimensions of different sections in the part can have a strong impact on the material properties and the machinability [1].

2.2. Phases and microstructure

In metallurgy, the term phase refers to a homogeneous state of matter. The phases differ from each other in chemical composition, type of atomic bonding and arrangement of elements, which phases, and in which quantities they are present in a metal, highly impacts the material properties. Iron-carbon alloys have four different phases; ferrite, austenite, cementite and δ-ferrite [4].

Phases can exist simultaneously, in grey cast iron the microstructure is called pearlite, which consist of the phases ferrite and cementite. Each phase has its own material properties, in iron-alloys the ferrite-phase is soft and ductile and the cementite phase is hard and brittle. In pearlite, the two phases acts synergetic and results in material properties that are both harder than the ferrite phase and also more ductile than the cementite phase. The amount of carbon in an iron alloy is important in determining what quantities the phases will be present [5].

The pearlite microstructure is formed when the cooling process of the melt is slow [6]. Grey iron is, among other things, characterized by the presence of free forming carbon embedded in the microstructure, this carbon forms as graphite flakes in the metallic matrix. The graphite flakes increases the wear resistance of the grey iron but decreases the toughness. The graphite structure, as for the microstructure, has a heavy impact on the material properties [7].

2.3. Graphite structure

The graphite flakes, which have a three-dimensional shape, has a decisive impact on the properties and machinability of grey iron alloys. It increases the machinability by acting as a chip breaker and lubricator in the cutting process. The lubricating effect of the graphite flakes is also beneficial in some applications were the products are subjected to a high degree of wear. Mechanically the graphite flakes act as a stress raiser, which can initiate fracture in the matrix at high stresses, therefore grey iron has little elastic behavior and fails under tension with almost no plastic deformation. The graphite flakes also gives grey iron a high damping capacity. Many factors affects the graphite structure, including carbon content, alloying elements and cooling time [8].

The ISO-standard [9] lists the different standards of cast iron according to form, distribution and size of graphite structure. The material used at Volvo should have graphite form I and the distribution type A. In Figure 2-1 the different typess of graphite forms can be seen.

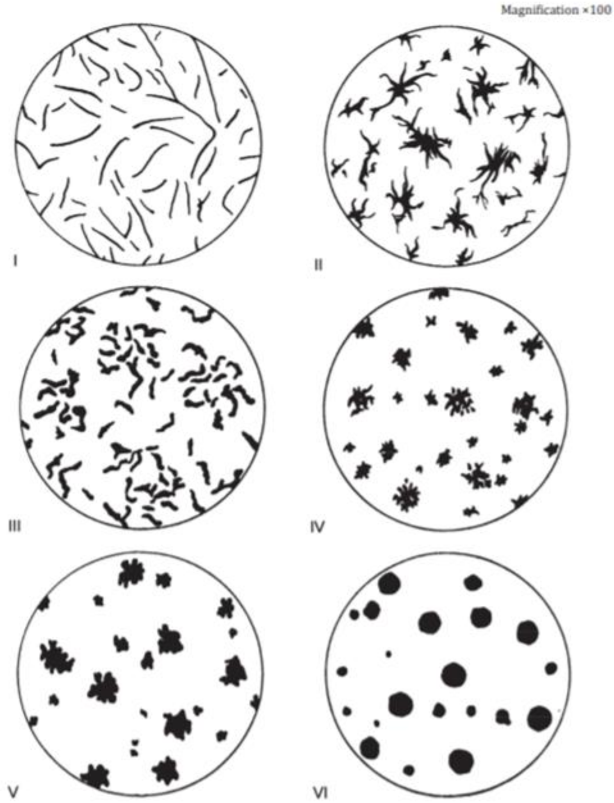

***Figure 2-1**: Different types of graphite form [9].*

Grey cast iron has a graphite formation of type I. [7]. The distribution of the graphite flakes can vary between the different types that can be seen in Figure 2-2.

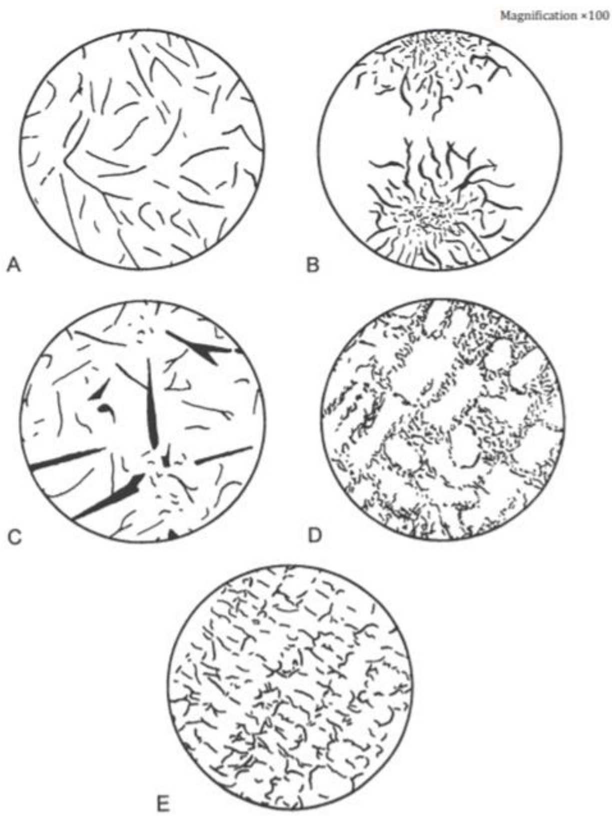

***Figure 2-2**: Types of graphite distribution in grey iron [9].*

Type A distribution is randomly distributed graphite flakes of roughly the same size. This type of graphite distribution is most often the desired one in engineering applications, mainly because of its superb wear resistant properties [10]. Type B graphite has a rosette like appearance. It is often the result of rapid cooling, common at thin section of casted parts [11].

Type C is characterized by its large graphite flakes and forms in hypereutectic irons. This type of distribution has a high resistance towards thermal chock, which is a result of increased thermal conductivity and decreased elastic modulus. The drawback of the large flakes are poor surface finish on machined parts, it also lowers the impact toughness and strength [11].

Type D has small interdendritic oriented graphite flakes. The formation of pearlite microstructure is often hard to obtained with this distribution, normally type D is formed in thin part of castings that has been subjected to rapid cooling. It may lead to increased tensile properties and often results in a higher degree of tool wear [10] [12].

Type E is similar to type D, having interdentritic oriented flakes. In type E the orientation is more uniform and forms in a ribbon like way. This distribution is undesired since it prevents the formation of pearlite microstructure and increases hardness and tensile properties, often resulting in a higher degree of tool wear [11] [12].

2.4. Alloying elements and their effect on grey cast iron

Alloying elements are used in grey cast iron to improve or alter the material properties in a desired way. For grey cast iron the most common alloying elements are carbon, which makes up for 2.5-4.0 wt%, and silicon, which is added in a quantity of 1.0-3.0 wt%. Silicon and nickel are graphite forming elements, especially silicon is of interest and is together with phosphorus used at the Volvo plant to calculate the carbon equivalent according to the formula in Equation 1-1 [13].

$$wt\%C + \frac{wt\%Si}{4} + \frac{P}{2} = Carbon\ equivalent \qquad \textit{Equation 1-1}$$

The carbon equivalent is often more useful and more easily calculated than the carbon content. Alloying a grey cast iron with phosphorus improves the fluidity by prolonging the solidification time, this facilitates the casting procedure by allowing the melt to reach all spaces in the mold [14]. Phosphorus also lowers the toughness of grey cast iron, this could be a desired feature since it improves the chip breaking during machining and reduces adhesion of workpiece material on the cutting tool edge [15].

Molybdenum is used to increase the strength at elevated temperatures and to reduce the risk of thermal fatigue. The same features as for molybdenum applies for chromium, however, this alloying element increases the risk of so-called white iron, which is hard and brittle and undesired and forms in corners and sharp edges of the cast part. To counter this, addition of copper is common when chromium is used, as it can neutralize the carbide stabilization of chromium [14].

Aluminum, titanium, vanadium and niobium act as grain refiners which improves the toughness of grey cast iron. This is most often undesired as it reduces the machinability. Hence, they are not added intentionally but can still be present since impurities and trace elements often are unavoidable in the melt. The exception is aluminum, which can be used as a nucleoid. [15].

Calcium and manganese act as sulfide formers when used as alloying elements. Sulfides are soft and lubricates the cutting process, thereby increasing the machinability [15]. As manganese sulfide inclusion have a higher thermal expansion coefficient than the iron matrix in grey cast iron, high tensions around the inclusion becomes present at elevated temperatures [16]. The tension enables the material to crack in the cutting zone during machining, which improves chip breaking and increases machinability. The lubricating features of the manganese sulfide inclusions reduce friction and heat generation at the tool-chip interface, which reduces tool wear, it can also act as a nucleoid during the solidification process [15].

2.5. Hard inclusions

Inclusions in a material can be either beneficial or harmful for the machinability. How they affect the machining process depends on numerous factors such as hardness of the inclusions, properties of the matrix material, chemical affinity with the cutting tool, type of machining operation etcetera. From a machinability perspective, inclusions can be beneficial in the following ways [16]:

- Facilitate chip breaking by acting as a stress raiser and thereby leading to brittle and easily broken chips.
- Form a diffusion barrier that protects the rake face of the tool from chemical wear.
- Lubricate the flank face of the cutting tool and thereby lowering the abrasive wear.

The main drawback with inclusions are the high hardness they possess. This is especially true for Rare-Earth-Metals that has a high affinity to impurities such as oxygen and nitrogen and easily forms as extremely hard inclusions. In some cases, the chemical composition of an inclusion could also be harmful for the cutting tool if it has a tendency to react to the coating material on the tool. Generally, the inclusions TiN or Ti(C,N) does not have any advantages to the machinability of a material. They are extremely hard and tend to cause a high degree of tool wear [16].

What impact inclusions have on the machining process depends on properties like size, morphology and concentration of the inclusions. The larger the inclusions are, and the higher the concentration, the heavier they will impact the machining process. This relationship work both ways, for example, if the inclusions causes tool wear, the tool wear will be increased if the inclusions are larger [16].

2.5.1. Titanium based inclusions

Although many inclusions, including Ti(C,N), are extremely hard (4200 – 4600 Hardness Vickers [17]), they could potentially lower the hardness and strength of the material they are encapsulated in. Ti(C,N) particles in ferrite materials can initiate cleavage fracture and thus lowering the strength and hardness. It has been suggested that this is caused by the difference in thermal expansion coefficient between the matrix material and the inclusions. The inclusions thereby induces tessellated stresses within the material and lowers the hardness and strength [18]. It has also been reported that the cutting forces decreases when the concentration of inclusions increases, although this decrease in cutting forces seldom leads to a reduction of the tool wear [19].

2.6. Oxides, nitrides, carbides and carbonitrides

Oxides, nitrides, carbides and carbonitrides can form inclusions within the grey cast iron. These inclusions are harder than the surrounding material and typically results in abrasive wear [20] Elements that typically forms oxides are aluminum, silicon, and calcium. Nitride forming elements include vanadium, niobium and titanium. Carbide forming elements are chromium, molybdenum, vanadium, tungsten, titanium and niobium. Carbonitride formers are vanadium niobium and titanium. These listed elements are often used as alloying elements in grey cast iron or can be present as undesired trace elements. For example are chromium and molybdenum used in small quantities in grey cast iron to reduce the graphite flake size and to refine the pearlite content. This improves the strength and ductility of the material. The higher the concentration of these elements are, the higher the concentration of oxides, nitrides carbides and carbonitrides [14].

2.7. Manufacturing of grey cast iron

Grey iron is manufactured by casting, which is an ancient method of metal forming. Casting involves pouring melted metal in a cavity called a mold in the shape of a desired part. When the metal solidifies, it is broken out of the mold and ready to be used or to be further processed [7].

There are many different methods and types of casting, the two main categories are casting in a single use molds and casting in permanent molds. Each with different advantages and disadvantages. The most common type of casting is sand casting, in which the mold is made out of sand. The advantage of this casting method is the relative cheapness of the sand molds and the ease, which these are produced. After the metal has solidified, it needs to undergo an after treatment. First, the casted part is broken out of the mold and excessive material is removed. The outer layer of the part is then often subjected to surface treatment in order to remove grades and traces of sand [7].

2.7.1. Machining

Milling is a manufacturing method in which a rotating multi cutting edge tool is moved and pressed towards a workpiece in order to remove material. In order for the milling process to be carried out the workpiece needs to be secured and fastened. This is typically done with clamps or fixtures. The milling process is intermittent, which means that the cutting edges are periodically engaged in the cutting of the workpiece. Milling therefor differs from turning where the engagement of the cutting edge normally is continuous and is carried out with a single cutting edge. Figure 2-3 shows two images of milling tools [20].

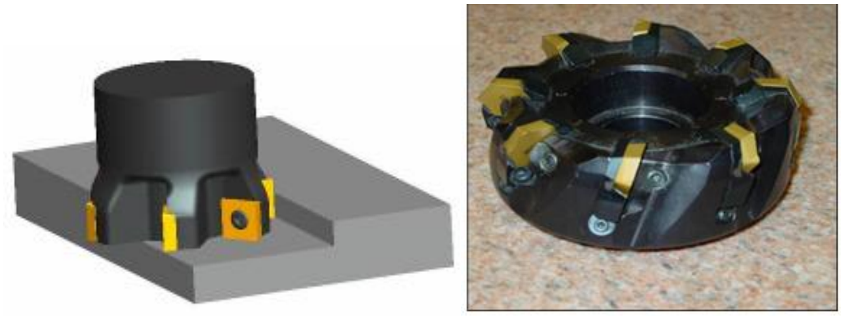

Figure 2-3*: To the left, a schematic illustration of a milling head. To the right, a picture of a milling head [20].*

2.8. The concept of machinability

Machinability is a broad concept with no clear definition. It depends on the combinations of multiple factors such as characteristics of the workpiece material, cutting data and the cutting tool properties. Machinability is however commonly described as:

" how readily a particular workpiece material can be machined by a cutting tool in a manner such that certain predetermined levels of form, size, and degree of roughness of the surface can be achieved." [1, page 389]

The level of machinability should therefore indicate how well a certain material can be expected to react during machining. This can be described as:

"Assessing the total costs of manufacturing a particular part in the manner aimed at, using the workpiece material in question"[1, page 389]

These definitions are not perfect since the costs are dependent on other factors such as the size of the series of parts that are to be manufactured or the geometrical shape or the demands on surface quality that are placed on the part. Figure 2-4 shows factors that affects the concept of machinability [1].

***Figure 2-4**: Factors that affect machinability [20].*

2.9. Workpiece materials and their machinability

This section will focus on the material factors that affects machinability. The most important material factors are listed below [1].

- Strain hardening.
- Adhesiveness.
- Specific heat and density.
- Microstructure.
- Ductility.
- Deformation resistance.
- Bulk hardness and distribution.
- Size of phases.
- Structure notch effects.
- size and geometric relations between η and β phases.
- Effect of epsilon-phases.
- Chemical reactiveness.
- Porosity.

These factors can be further divided into 5 purely material factors. These factors can, singly or in combination with each other, impact the machinability of a workpiece material. The 5 factors are:

- Hardness and deformation resistance
- Abrasiveness and proneness to wear
- Ductility
- Strain hardening
- Thermal conductivity

The potential machinability of a material can be assessed with these factors but cannot explain it completely. Other material factors such as adhesiveness, chemical reactivity and diffusion could also have a decisive impact on the machinability. However, those factors are often very specific and are not easily described in general terms. Chemical reactivity for example is only harmful to a cutting process if the machining is carried out with a cutting tool material that is reactive to the workpiece material in question [1].

A so called polar diagram can be made to visualize the impact on the machinability by the 5 main material factors. A polar diagram of the machinability of grey cast iron can be seen in Figure 2-5. The scale of a polar diagram is relative and can be used in comparison of different materials [1].

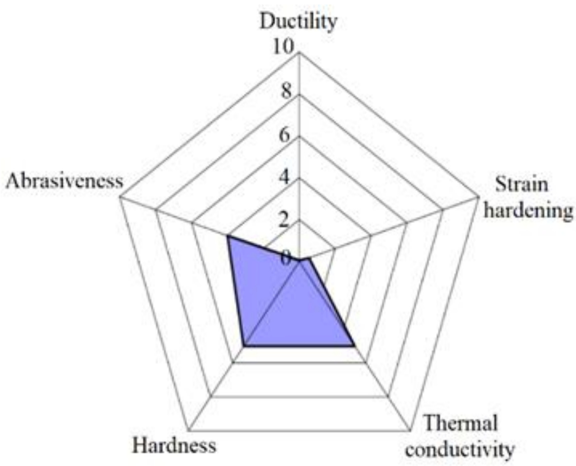

Figure 2-5*: Polar diagram of the machinability of grey iron with the five main factors that affects the machinability of a workpiece material [20].*

2.9.1. Strain hardening

Strain-hardening is a hardening of the outer layer of the workpiece material that has undergone machining. This outer layer often has considerably higher hardness and yield strength than the material that has not been machined. Strain hardening is undesirable and increases the load on the cutting edge and thereby the risk of plastic deformation of the cutting tool. If strain hardening is combined with low thermal conductivity the machinability of the material will be rather low [1].

2.9.2. Ductility

Ductility describes the ability of a material to withstand a high degree of plastic deformation without breaking. In some applications, it could also complicate the chip breaking process and produce undesired long chips. High ductility often corresponds to high adhesiveness, this is the tendency of a workpiece material to adhere to the cutting tool. Adhesiveness can be both an advantage and a disadvantage. Under some circumstances, workpiece material can adhere to the cutting tool and form a protective layer on the cutting edge. If the adhered workpiece material is not stable and is frequently removed from the cutting tool, this can lead to rapid adhesive wear [1].

2.9.3. Abrasiveness

Abrasiveness is not as easily quantified as the other five material factors. It can not be described in a clearly physical term as for example thermal conductivity (Wm-1K-1) or hardness (Brinell, Vickers etc.). Instead, it needs to be quantified by calculating a composite score based on the micro hardness of the workpiece material, the difference in hardness between the materials structural phases and on the shape, size and hardness of the inclusions in the material. The quantity of the alloying elements a material contains can be a factor that determines the degree of abrasiveness. If these elements are prone to form hard carbides and oxides, the abrasiveness will increase [1].

2.9.4. Hardness

The hardness of a material is linked to the deformations resistance. High deformation resistance leads to high cutting resistance. Thus, a hard material creates a high cutting tool load. A material with varying hardness also creates variances in the cutting forces, this leads to a short-chipping material that creates segmented chips. Hardness is only a measure of machinability when comparing materials that are otherwise similar in their characteristics [1].

2.9.5. Thermal conductivity

During machining, the movement between the workpiece and the cutting tool creates friction which generates heat. If a workpiece material has a low thermal conductivity the level of heat conduction that takes place will be low and the heat will largely be transferred into the cutting edge resulting in a low machinability. In materials with good thermal conductivity the heat that is generated in the cutting process will be transported out of the cutting zone into the surroundings, in particular with the produced chips. The better the thermal conductivity, the higher the cutting speed can be without overheating the cutting process [1].

2.10. Cutting tools

The purpose of a cutting tool is to remove material from the workpiece by deformation and shearing. Cutting tools can be divided into two groups. Solid cutting tools and cutting tools with indexable inserts. In this study cutting tools with indexable inserts are being used. Often the cutting edge of a cutting tool is provided with a hard coating to protect it from different types of wear [1].

Cutting tool geometry is the form and dimensions of a cutting tool. In order to describe various types of wear or operation settings the different surfaces or angles are often referred to. The geometry of a cutting tool highly affects the cutting process and choosing the right geometry is crucial to obtain an optimal result. In Figure 2-6 the basic geometries of a cutting tool is schematically illustrated [20].

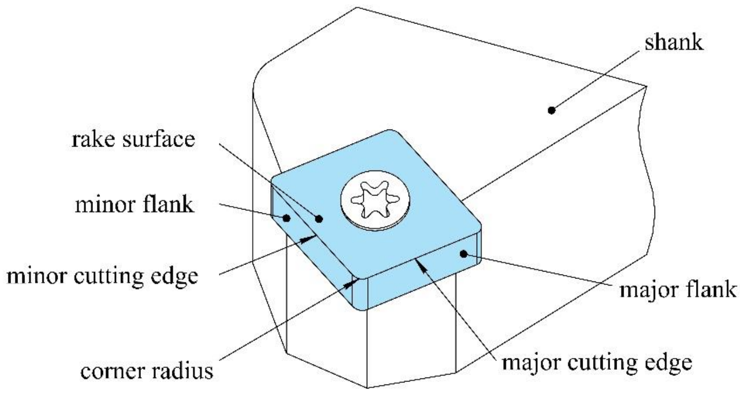

Figure 2-6*: Schematic illustration of a cutting tool and a cutting tool holder [20].*

The shank holds the cutting edge in place, offers support during machining, and connects the cutting edge to the machine. The cutting edge is the part of the cutting tool that is most subjected to wear and forms in the intersection of the rake surface and the flank surface. During cutting, the chips will glide over the rake surface. The flank surface is the part of the tool that is faced towards the workpiece. The cutting tip is formed at the junction of the main and the minor cutting edge and can be either sharp or rounded. If the cutting tip is rounded, the size of the radius is called nose radius [1].

The cutting tool material has a decisive impact on the cutting performance of a tool. Cutting tools deteriorate when they are used. To tackle this there is some main required properties the cutting tool material needs to possess [20].

- Hardness or wear resistance. This influence the ability of the cutting tool to withstand the abrasive wear that occurs in contact with the workpiece material. A minimal requirement in order for the cutting tool to function is that it is harder than the material that is machined. With low hardness the cutting tool will wear out quickly. Hot hardness is the ability to maintain hardness during the high temperatures that can develop during machining [20].

- Toughness is the ability to withstand mechanical shock. This is especially important in intermittent cutting like milling. Toughness and hardness are dependent on each other. If a material is very hard it is also becomes brittle, the opposite to though, and more prone to breakage. Thermal shock resistance is also a desirable material property of cutting tools [20].
- Chemical inertness. This is the ability to chemical wear and diffusion that can take place between the cutting tool material and the workpiece material [20].

2.10.1. Coatings

To increase the wear resistance a protective layer, a coating, can be applied to the cutting tool. The coating is usually composed of some sort of ceramic, although diamond or diamond-like materials is also used. The ceramics that are being used include carbides, oxides and nitrides. These materials are characterized by their ability to being stable at high temperature, being chemically inert and their hardness and brittleness. The coatings are applied to cutting edge as a thin layer which allows the toughness of the bulk material in the cutting edge to be combined with the desirable features of the ceramic without suffering from their drawbacks (like brittleness) [1].

Coatings is applied on the cutting edge with either of two methods. A thin coating (1 – 5 µm) is applied by the Physical Vapor Deposition (PVD) technique and thicker coating (4 – 20 µm) uses the Chemical Vapor Deposition (CVD) technique. Commonly used materials that are applied as coating with the PVD technique includes titanium, aluminum, chromium, silicon, oxygen and nitrogen. Coatings that are applied with CVD technique most often uses titanium carbonitride Ti(C,N), Titanium nitride TiN and Aluminum oxide Al_2O_3 [20].

2.11. Cutting tool deterioration

The machining cost is greatly affected by the types of wear or deterioration the cutting tool is subjected to and the speed at which this occurs. During machining, the cutting tool is subjected to a range of different loads including tribological, mechanical, thermal and chemical loads. These loads will in turn cause wear on the tool, mainly on those areas on the cutting tool that are in contact with the workpiece. The deterioration of the cutting tool is what decides the tool life, when the deterioration reach such proportions that the tool can no longer sufficiently function during a machining operation it must be replaced. Generally, the wear will increase when the productivity of a machining operations increases (e.g. by increasing the cutting speed) [20].

Below is a list of the different types of cutting tool deteriorations [20].

- Wear: Continual loss of material from the cutting tool that causes changes in the tool geometry.
- Plastic deformation: Changes in the tool geometry without the loss of material.
- Breaking and cracking: Crack formation or sudden loss of material in the form of flaking, chipping or tool failure.
- Material transformation: Changes in the tool material structure or characteristics due to chemical processes like diffusion or chemical reactions.

Which type of deterioration that will be predominant depends on multiple factors including tool material, cutting data and conditions and workpiece material. These results in different types of wear and are described in what follows [20].

2.11.1. Abrasive wear

Abrasion is the deterioration of a material by scratching, wearing or grinding and is a frictional process that takes place on the rake face of the cutting tool where it is in contact with the chips or on the clearance face that is in contact with the machined surface of the workpiece material. As illustrated in Figure 2-7 the abrasive wear in a metal cutting process can be caused either by direct contact between the cutting tool and the workpiece material or by small particles present in the workpiece material, so called hard inclusions. If the wear is not caused by hard inclusions, it is often called erosive wear. Abrasive wear is much more common in materials with hard inclusions or in materials with a hard surface layer. Hard surface layers are often associated with casted materials. The surface, or the cast skin, can consist of hard carbides or contain traces of foundry sand. Hard inclusions tends to consist of oxides, carbides or nitrides [1].

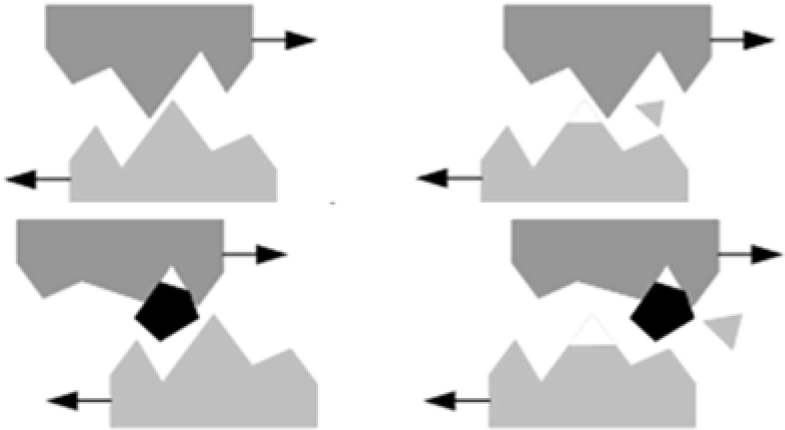

Figure 2-7*: Abrasive wear caused by grinding between the cutting tool and the workpiece (top) and by the presence of hard inclusions (bottom) [20].*

2.11.2. Adhesive wear

Adhesive wear occurs when workpiece material is welded to the cutting edge by the high temperature and pressure in the cutting process. This adhered metal is referred to as a built-up edge (BUE). The adhered material will sooner or later break of and cause micro-chipping of the cutting edge. Another problem with BUE is its hardness, which is considerably harder than the workpiece material and can lead to a reduction of the quality of the machined surface [20].

2.11.3. Flank wear

Flank wear has the appearance of a relatively uniform abrasion along the cutting edge, see Figure 2-8, and is the most desired type of wear due to its predictability. The wear surface is parallel to the cutting speed direction and as the wear surface increases the cutting edge will become blunt and the clearance angle will approach zero. As a consequence of this the shear forces and the normal forces will increase as well as the heat generation and the cutting resistance. If the flank wear is progressed long enough the position of the edge line in relation to the workpiece will shift successively which needs to be compensated for if the geometrical dimensions of the manufactured parts are to be met [1].

Figure 2-8*: Typical appearance of flank wear on a cutting edge [21].*

2.11.4. Crater wear

At higher cutting speeds, crater wear is a combination of diffusion and decomposition. At lower cutting speeds it is caused by abrasive wear. Crater wear takes place at the rake face of the cutting tool, see Figure 2-9. The wear surface is usually not directly on the edge line. Crater wear occurs when the heat from the workpiece chips decomposes the tungsten carbide grains in the substrate. Carbon will then diffuse into the chips and cause a wear in the form of a crater on the rake face of the cutting tool. Crater wear will reduce the wedge angle, which will weaken the cutting edge, a weakened cutting edge will then in turn increase the risk to more severe chipping or even fracture [1].

Figure 2-9*: Crater wear on the rake side of the tool. Note that the schematic sketch is turned 90 degrees in relation to the picture of the cutting tool [20].*

2.11.5. Notch wear

Notch wear usually occurs on the clearance face of the tool in the area where the contact between the workpiece chips and the cutting tool ceases. The temperature in this area of the tool is very high and it is also in contact with the oxygen in the surrounding air. The combination of heat and access to oxygen causes oxidation of the cutting tool material and is then easily worn off. A cast skin increases the risk of notch wear [20].

2.11.6. Plastic deformation

Plastic deformation is a change in the geometry of a cutting tool without any loss of material. It occurs when the combination of thermal and mechanical loads reach a critical level. High temperatures causes the carbide binder of the cutting tool to soften, the pressure from the mechanical loads will then plastically deform the cutting edge. Since flank wear increases the normal and shear forces plastic deformation often arises in combination with flank wear. Two basic types of plastic deformation can be distinguished, as shown in Figure 2-10. The tangential loads is predominant in case A, whereas the axial and radial loads are higher for case B [1].

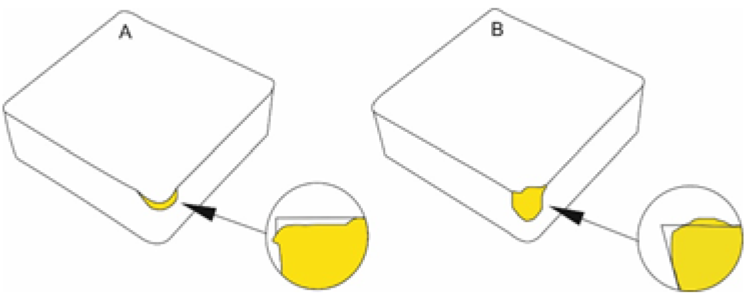

***Figure 2-10**: Plastic deformation of type A and type B [20].*

2.11.7. Chipping and fracture

Chipping and fracture is the breakout of material from the cutting tool. The difference between chipping and fracture is the severeness of the damage. With chipping, the cutting tool can still be used whereas fracture makes further use of the cutting tool impossible. There is no exact definition of the two concepts since different applications can tolerate different extent of chipping. Chipping and fracture occurs on the edge line of the cutting tool where there is contact with the workpiece. Chipping can be caused by many different factors but is often a result of fatigue from cyclical loading, which is often associated with intermittent cutting like milling. Cracks and chip hammering could also weaken the cutting tool and make it more likely to experience chipping. Figure 2-11 displays chipping of a cutting edge that has been initiated by thermal cracks. Chipping affects the surface quality, for roughing operations where the demand for surface quality is rather low a higher tolerance for chipping can be accepted [1].

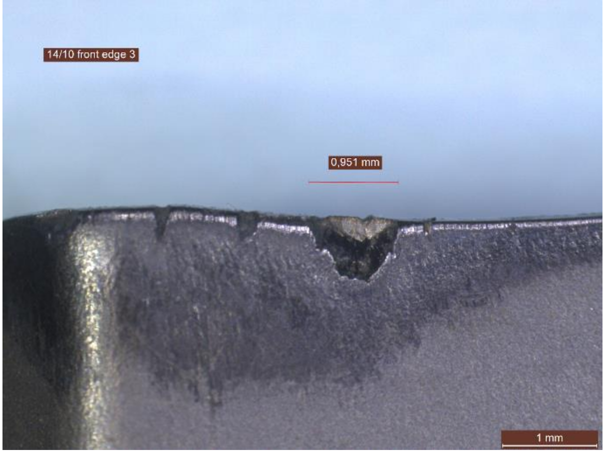

Figure 2-11*: Chipping of a cutting initiated by thermal cracks. The picture was captured in this study.*

2.11.8. Thermal cracks

Thermal cracks are caused by a combination of thermal cycling (periodically changing temperatures), thermal loads (temperatures differences between different areas in the cutting tool) and mechanical shocks. The cracks appear along the edge line as can be seen in Figure 2-12. The cracks will cause sections of the cutting edge to wear out and will eventually lead to chipping since it weakens the cutting edge. This type of wear occurs mostly in milling since intermittent operations are causing thermal cycling and mechanical chocks [1].

To counter thermal cracks a tougher cutting tool material can be used. Correctly applied coolant could also be an effective method, however this is riskful since it could increase the difference in temperature between areas in the cutting tool and enhance the thermal cycling [1].

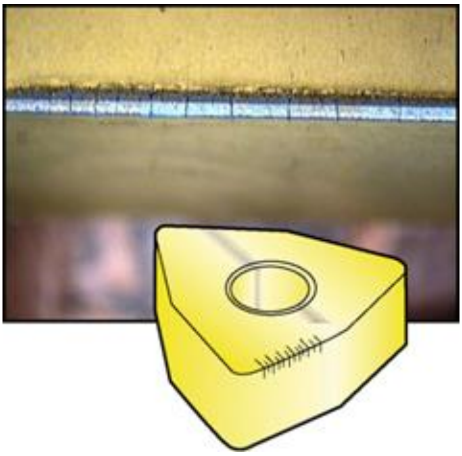

Figure 2-12: *Thermal cracks on a cutting edge [20].*

2.11.9. Diffusion

Diffusion is a process where material is exchanged between the cutting tool and the workpiece material at an atomic level. This loss or change in the cutting tool material weakens the tool and makes it more prone to other types of deterioration. Diffusion is highly temperature-dependent and becomes a serious problem for cemented carbide grades at 800-1100 °C. In the metal cutting of ferrite materials such as steel and cast iron diffusive deterioration takes place when Fe atoms from the workpiece diffuse into the cemented carbide of the cutting tool. The relatively mobile carbon atoms in tungsten carbides can also diffuse into the workpiece. A coating on the cutting tool can act as a barrier to hinder diffusion between the workpiece and the cutting tool [1].

2.11.10. Chemical wear

Cemented carbides can oxidize at temperatures of 800 deg° C if oxygen is available. In continuous cutting operations, there are not enough oxygen between the workpiece and the chips for oxidation to take place, in intermittent cutting however there are. Oxidation weakens the cutting tool and makes it more prone to other types of deterioration [1].

2.12. Testing methods

Testing methods in this study are used to evaluate certain material properties of grey cast iron. In what follows is a short presentation of the Brinell hardness test and the functioning of a scanning electron microscope used to determine the chemical composition of inclusions found in the workpiece material.

2.12.1. Brinell hardness test

Hardness can be measured in numerous ways. Common type of hardness tests include Vickers, Rockwell and Brinell. These tests have in common that they all use an indenter and an implied load to create an indentation in the material that are being tested. The smaller the indentation the harder the material is [22].

The Brinell hardness test is a none-destructive method that are used to test material that have coarse structures or surfaces, for example castings and forgings. By using a indenter that have a wide surface area and a high test load the resulting indentation averages out surface or structural inconsistencies. In Figure 2-13 a schematic image of a Brinell hardness test is shown. A predetermined test load (P) is applied to a hardened steel ball of fixed diameter (D) which is held for a predetermined time period and then removed. The resulting indentation diameter (d) is measured and used to calculate the Brinell hardness number (BHN) [22].

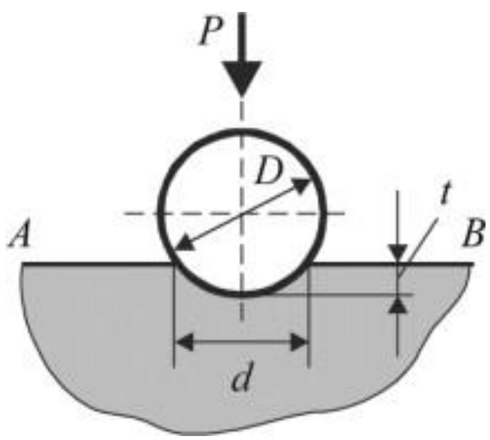

Figure 2-13*: Schematic illustration of a Brinell hardness test [22].*

To calculate the Brinell hardness number Equation 1-2 is used.

$$BHN = \frac{2P}{\pi D(D-\sqrt{D-d})} \qquad \textit{Equation 1-2}$$

2.12.2. SEM-XEDS

A scanning electron microscope (SEM) is a type of electron microscope that creates magnified images of a material sample by scanning it with a focused beam of electrons. When the beam of electrons hits the atoms in the material sample a number of interactions take place which can be detected and in turn generate useful information of the structure and composition of the material sample. Figure 2-14 shows a schematic picture of a SEM [14].

While SEM is used to observe objects that are too small to be viewed by conventional optical microscopes Energy-dispersive X-ray spectroscopy (XEDS) are useful in determine the chemical composition of studied samples. The XEDS analyzes the interaction between X-rays and the material sample by utilizing the principle that every element has a unique atomic structure, which has a unique set of peaks on its electromagnetic emission spectrum. When the X-ray beam hits the material sample, electrons in the inner shell is ejected and creates an electron hole. This will make a more energy dense electron from an outer shell take its place. When the excessive energy from the outer shell electron is released in form of an X-ray. The energy from the X-rays can then be measured and analyzed to give information of the chemical composition of the studied samples [14].

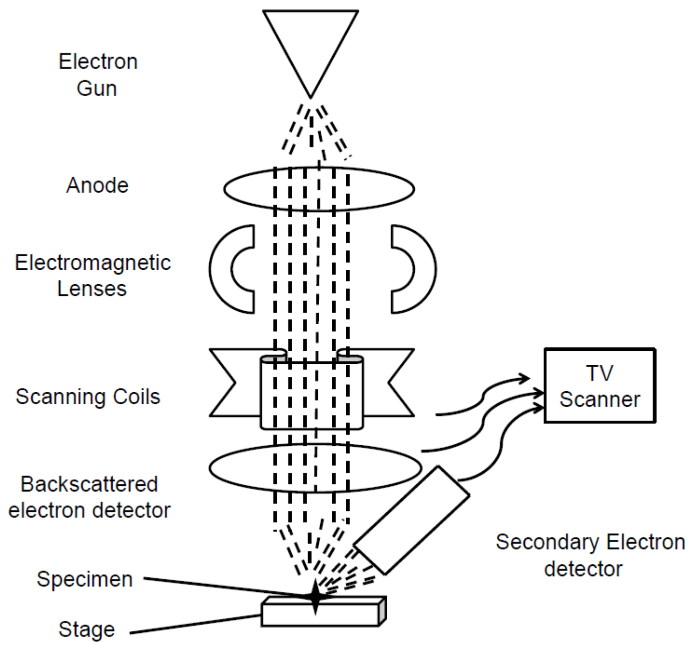

Figure 2-14: *Schematic illustration of a SEM [23].*

3. Method

In this chapter the methods used for collecting and analyzing data is presented. Data was collected in three different ways. By collecting cutting tools used in the production of the engine blocks, by acquiring chemical analyzes from the foundry of those engine blocks that were machined by the collected tools and finally by extracting material samples from said blocks. Ten series of inserts and chemical analyzes and five material samples were collected. The cutting tools were examined in a microscope and the type and degree of wear was recorded. The graphite structure, the hardness and the concentration of inclusions were examined in the material samples. The chemical analyzes were used to compare the chemical composition in engine blocks.

3.1. Workpiece material

The products that are being machined are the 11-liters engine block for Volvo trucks that is displayed in Figure 3-1. The engine block weighs 245 kg when it enters the production line and 48.3 kg of material has been removed when it exits the production line. The material used in the engine blocks are grey cast iron that has been cast in house.

***Figure 3-1**: An example of an engine block studied in this report.*

3.2. Machining and cutting data

Cutting tools were collected from a milling machine at the workstation OP20. Three different surfaces of the engine block are machined in OP20, the top and the two gables.

The top undergoes four sweeps and the gables only one sweep. The cutting data differs slightly between the different sides of the engine block. Table 3-1 presents the cutting data for the three sides.

***Table 3-1**: Cutting data.*

Cutting data	Gable 1	Top	Gable 2
Cutting speed [m/min]	250	250	250
Revolutions per minute [rpm]	398	398	398
Feed per revolution [mm/rev]	6.5	8.3	7
Feed per insert [mm/insert]	0.20	0.26	0.22
Feed [mm/m]	2600	3300	2800
Cutting depth [mm]	4.00	2.50	4.00

3.3. Cutting tools

The cutting tools used in this study are delivered from the cutting tool manufacturer Walter's Nordic department and has the XNMF090612-D27 WKP25S tool geometry. The cutting tool is a double sided heptagonal cemented carbide insert with an aluminum oxide coating called CVD Tiger-Tec silver [24]. Aluminum oxide has a Hardness Vickers of about 2000 [25].The cutting tool can be seen in Figure 3-2 and the dimensions are presented in Table 3-2.

__Table 3-2__: Proportions of the cutting tools.

Cutting tool data		
Diameter of inscribed circle	d	19.05 mm
Cutting edge length	l	9 mm
Insert thickness	s	5.67 mm
Corner radius	r	1.2 mm

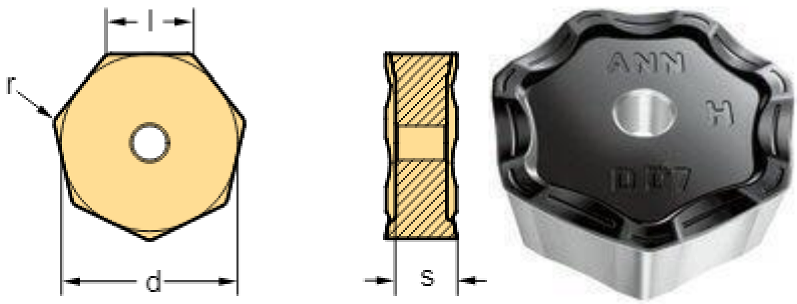

__Figure 3-2__: To the left, a schematic view of the cutting inserts studied in this report. To the right, a picture of the same __[24]__.

3.4. Collection of cutting tools

Cutting edges are replaced after they have been used in the machining of 100 engine blocks or when the operators consider them to be worn out. The choice of 100 blocks before replacement is rather conservative; the purpose of this is to add a safety factor to avoid unwanted production disturbances and cassations. During this study, only one series of cutting inserts was collected who had been used in less than the machining of 100 blocks. In the first series six inserts were collected, and ten inserts were collected in the other nine series.

Optimally, the cutting inserts that were to be collected should machine 100 blocks that were cast in a sequence directly after one another, this to assure that the material would be as consistent as possible and to attain a more precise chemical analysis from the foundry. This was done for the two first collected series of cutting inserts. This method was later abandoned due to the time consuming procedure of marking sequent casted engine blocks and the cost and inconvenience of planning the production in this manner.

In test series 3-10, the inserts were collected under normal production conditions. The production line does not machine the blocks in any specified order, they simply use the material that is delivered from the foundry. This means that blocks that are casted in different days can be machined with the same inserts. This would obviously make the evaluation of the wear on the inserts useless if the aim is to examine the casted materials impact on the tool wear. To avoid this, the storage area for incoming blocks from the foundry were inspected every morning, and by checking the date and time mark on the blocks it could be determined if they had been casted the same day and if so inserts could be collected that day.

3.5. Collection of chemical analyzes

To collect chemical analyzes, the date and time mark on the blocks that were machined during a test series were recorded and later obtained from the foundry's digital archive where those analyzes were kept. Since test series 3-10 was not as precise as series 1 and 2, the chemical analyzes of those series are an average of the chemical composition of all blocks that were produced that day and not for exactly those 100 blocks that were machined.

3.5.1. Evaluation of chemical analyzes

The exact chemical composition of the grey cast iron in the engine blocks are classified. To prevent the reveal of this the variation of chemical content are presented as the percentage of the average of all engine blocks.

The elements detected in the chemical analyzes are divided in four groups. The first three groups are carbide-forming elements, oxide-forming elements, and the carbon equivalent. All elements that do not fit in any of these three groups are labeled as other elements.

3.6. Collection of material samples

Engine blocks from five different test series were collected as material samples. The blocks were chosen at random in the production series were cutting tools had been collected. A so-called destructive test were the gables were sawn off had to be done in order to examine the material sample.

In all five collected engine blocks, the material samples were taken from the gables. In the first two collected blocks, four pieces of material samples were taken. Two from the top surface of the gable and two from the side surface. In Figure 3-3 the gable can be seen, the yellow markings indicate where the material samples were taken from the two first blocks. In the last three blocks one sample from the top surface were taken from each gable and one sample from bulk material about 10 millimeters below the surface.

Figure 3-3: *Sawed of gable used in a destructive test. The yellow markings indicate where the material sample were taken in engine block 1 and 2.*

3.7. Material preparations

The material samples were mounted in epoxy like the one that can be seen in Figure 3-4. The mounting enables the material samples to be easier polished and studied in microscopes.

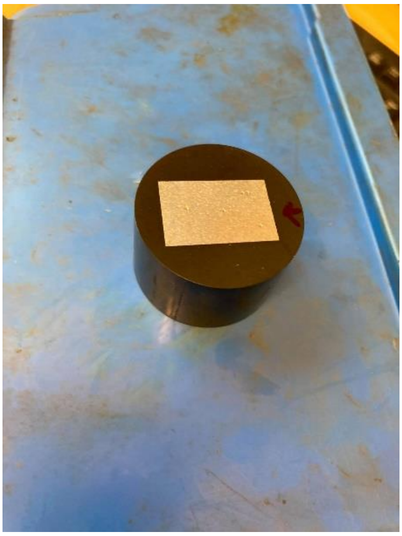

Figure 3-4: *Material sample mounted in epoxy.*

The mounts were first polished so the graphite structure could be studied in microscope. After this, the samples underwent etching to enhance the visibility of the microstructure and the titanium carbonitrides The etching was done with a 2% solution of nital.

3.8. Evaluation of cutting tool wear

To evaluate the wear of the collected inserts, a wear classification system was set up. Each insert is graded from 1 to 4 according to the severeness of the edge wear. Level 1 indicates the least amount of wear and level 4 the most. Level 2 is regarded as the normal amount of wear that can be expected. What follows is a presentation and explanation of the level of wear that the cutting edge can be assigned. Each level is exemplified by a picture of a cutting tool taken in this study, for reference an unused insert is shown in Figure 3-5. The wear was evaluated with the help of a microscope with a magnification of times 40, every picture contains a scale bar for comparison.

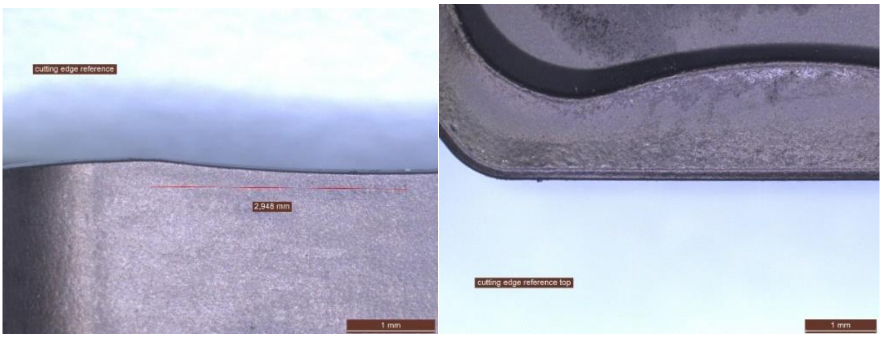

Figure 3-5*: An unused cutting edge.*

3.8.1. Tool wear degree 1

At this degree there is not much wear on the cutting edge. Small signs of incipient comb cracks can be seen. Figure 3-6 shows a cutting edge with wear degree 1.

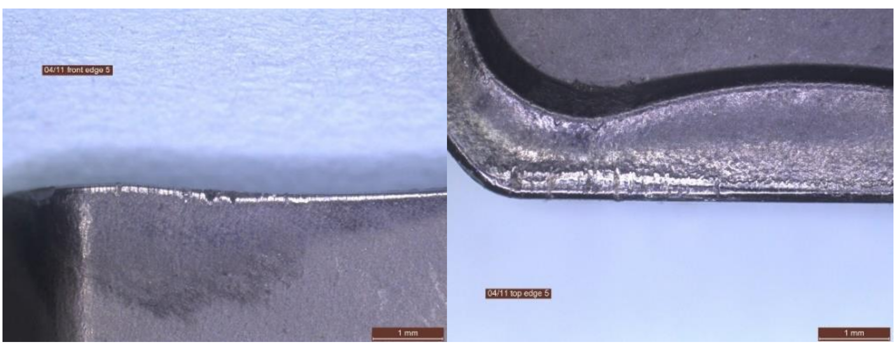

Figure 3-6*: Example of a cutting edge with tool wear degree 1. Incipient thermal cracks on a cutting edge can be seen.*

3.8.2. Tool wear degree 2

The thermal cracks at this degree of wear are deeper and wider than in degree 1. Small chipping of the edge line can be present. Figure 3-7 shows a cutting edge with wear degree 2.

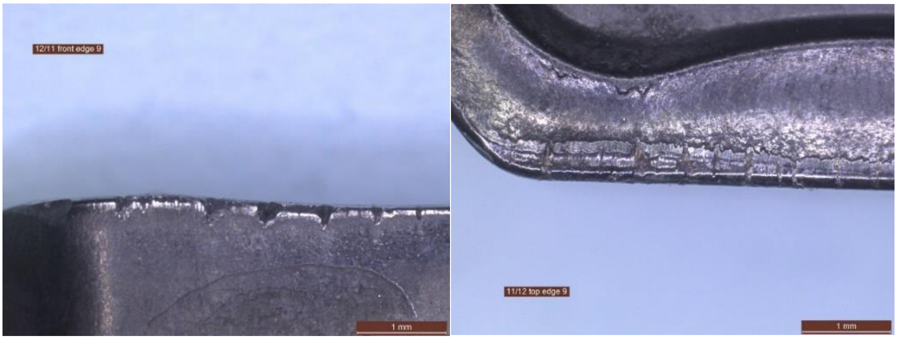

***Figure 3-7**: A cutting edge with tool wear degree 2. Comb cracks are deeper and some damage to the cutting tip can may have happened.*

3.8.3. Tool wear degree 3

At this degree, the chipping is more severe with chunks of the metal broken out of the matrix. Figure 3-8 displays an insert with tool wear degree 3.

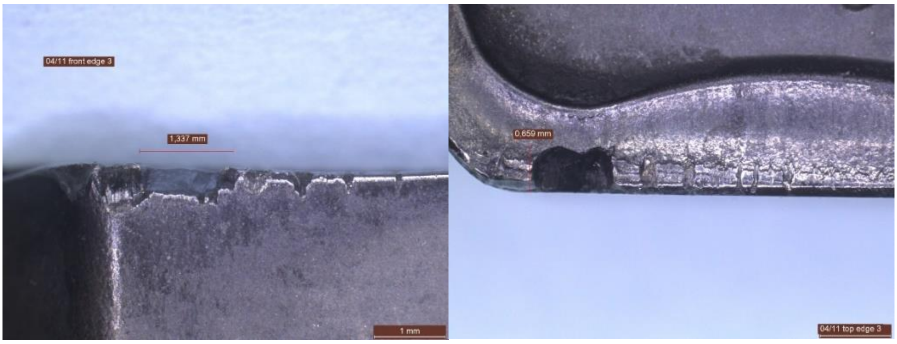

***Figure 3-8**: Insert with tool wear degree 3. Parts of the edge has been broken off*

3.8.4. Tool wear degree 4

At this degree, big parts of the edge are heavily damaged in more than one place or in a very large section of the edge. Figure 3-9 displays a tool wear of degree 4.

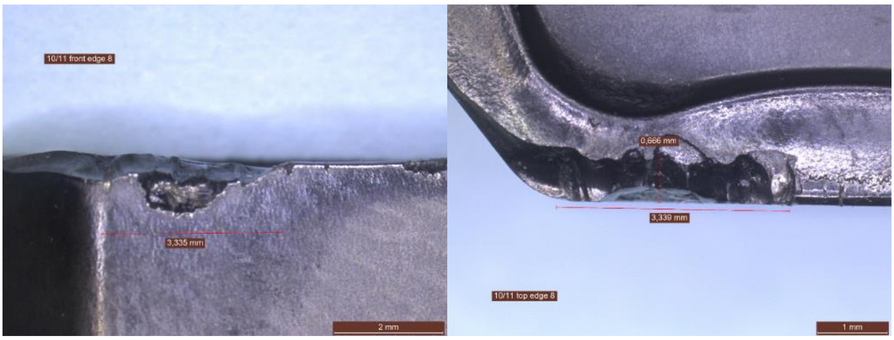

Figure 3-9*: Insert with tool wear degree 3. The cutting edge has suffered severe damage and is practically unusable.*

3.9. Evaluation of graphite structure

The polished material samples were examined optically in a microscope with a magnification of times 50 at the top, middle and bottom of the sample to analyze the graphite structure. The top of the sample is the part that is closest to the sharp edge of the engine block. For clarification se Figure 3-10 below. After the microscopic examination a picture was taken of a representative area of the sample at the top, middle and bottom at magnification of times 50. The graphite structure was then classified according to the ISO-standard.

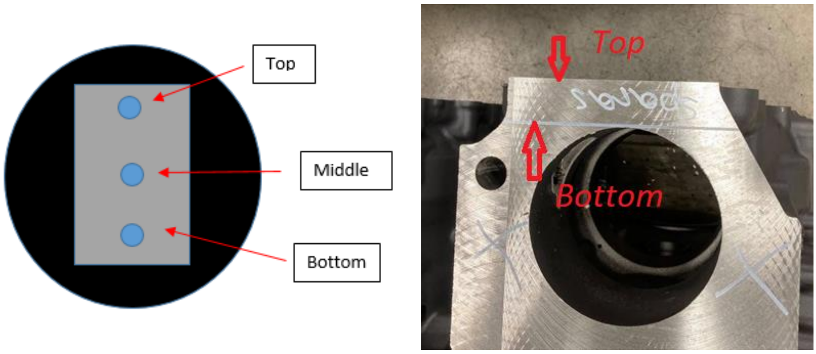

***Figure 3-10**: Schematic illustration of the material samples (left) and the corresponding area at the engine block (right).*

3.10. Inclusions

The hard inclusions in the material were assessed in four categories. Concentration, size, morphology, and distribution. They are further explained in the text that follows.

3.10.1. Concentration

The concentration of inclusions were measured in relative terms between the samples by counting the number of inclusions within a fixed area. The microscope was set to a magnification of 500X and the counting started at the top of every material sample. While the microscope was fixed horizontally every inclusion along a vertical 10 mm path in the focus of the microscope were counted. At this magnification the width of the focus is 165 µm, the width times the length 10 mm gives an examined area of 1.65 mm^2. Figure 3-11 shows a schematic model of how the tests was conducted.

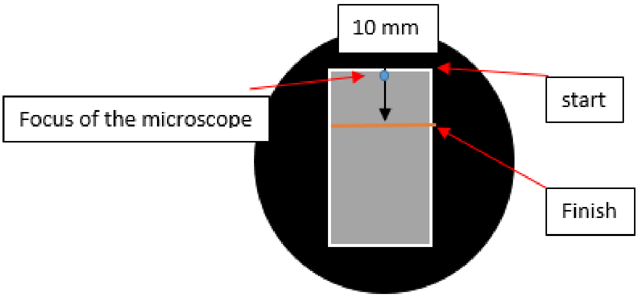

Figure 3-11*: The focus of the microscope was fixed horizontally while every inclusion along a 10 mm path of the material sample were counted.*

3.10.2. Size

The inclusions were divided into three groups: small, medium and large. An inclusion was categorized as small if its largest side was less than 2 µm in length and large if the largest side were over 5 µm in length. Any inclusion with a largest side between those values was categorized as medium. It should be noted that the length of the inclusions are estimations since every inclusions cannot be measured and the geometry of the inclusions are not always easily measured.

The somewhat vague terms small, medium, and large were only set up for use in this study. They do not reflect the size of other types of inclusion than those studied in this report.

3.10.3. Morphology and distribution

Since the geometrical shape of the studied inclusions with very few exceptions where quadratic or rhombic with sharp edges there were no need to categorize them according to morphology. In the distribution however, a significant number of the titanium-based inclusions were nucleated to a manganese sulfide inclusion, hence the titanium carbides were in addition to size also labeled as either nucleated or detached.

3.10.4. Chemical composition

The inclusions were examined with a field emission scanning electron microscopy (SEM) equipped with an X-ray energy-dispersive spectrometer (XEDS) located at the department of geology at Lund University to determine which elements they were composed of. Several inclusions of varying shape and size were examined.

3.11. Hardness

The hardness was evaluated by the use of the Brinell hardness test. The load was 287.5 kg and the hardened steel testing ball had a diameter of 2.5 mm. Three tests were conducted on every material samples. Each on roughly the same place as were the graphite structure were examined, namely top, middle and bottom.

4. Results

In this chapter, the results from the tests and examinations are presented. Including the composition and concentration of inclusions, the graphite structure and the hardness of the material, and the variation of chemical composition in the different series of engine blocks. Photographs of the graphite structure of the material samples and typical wear patterns on the cutting tools are also presented.

4.1. Evaluation of inclusion composition

Figure 4-1 shows an SEM image of an inclusion found in the top area of the surface material from block 3. The white square marked as Spectrum 7 indicates were the XEDS analysis was done.

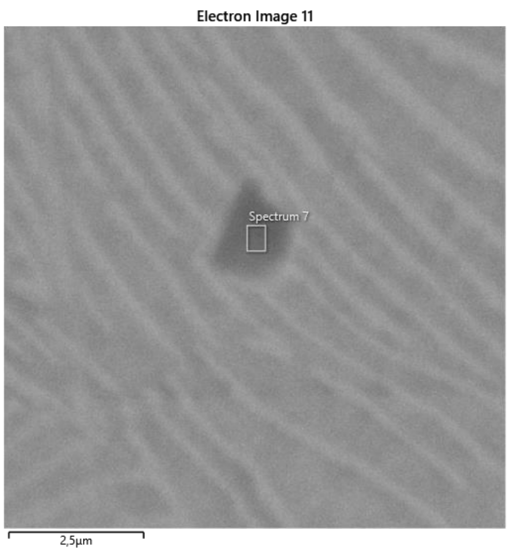

Figure 4-1: *Inclusion analyzed in the SEM.*

Table 4-1 shows the chemical composition of Spectrum 7. Carbon, nitrogen, titanium, and iron are the dominating elements. Based on the composition in the table and the fact that XEDS results has a tendency to be influenced by the underlying material and to overrate light elements such as carbon an nitrogen, the inclusion seen in Figure 4-1 is with high certainty made of titanium carbide nitride Ti(C,N).

Table 4-1:*Elements found in Spectrum 7*

Element	Atomic %
C	33.76
N	22.60
Si	0.58
Ti	14.98
V	1.55
Cr	1.13
Fe	21.31
Nb	3.10
Mo	0.99
Total:	100.00

Figure 4-2 shows a SEM-image in the same areas as Figure 4-2. The inclusions shown here are considerably larger than in the first SEM-image (note the scale bar in the images). Four sites of XEDS analyzes of the material was done, indicated in the picture as spectrum numbered 1-4. In addition one general analyze of the area visible area in Figure 4-2 was done were the frequency of a number of elements are shown.

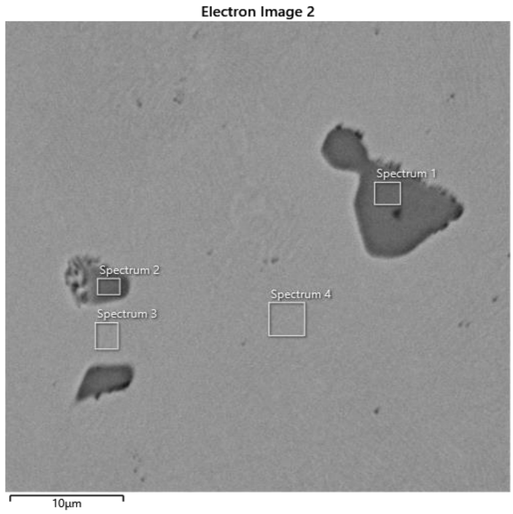

***Figure 4-2**: SEM-image of grey cast iron and three inclusions. The white squares indicates were XEDS analyzes have been made.*

The chemical composition of Spectrum 4 is presented in Table 4-2. The analyzed area is from the matrix material, i.e. the grey iron. Iron and carbon is the dominating elements, once again it is obvious that the SEM-analyze tends to overrate lighter elements such as carbon in this case.

***Table 4-2**: Elements found in Spectrum 4*

Element	Atomic %
C	31.81
Si	2.47
P	0.21
Cr	0.45
Mn	0.52
Fe	64.27
Cu	0.27
Total:	100.00

Table 4-3 presents the chemical composition of the top left inclusion labeled Spectrum 2. Dominating materials are carbon, sulfur, manganese and iron, which strongly indicates that the inclusion are a manganese sulfide.

***Table 4-3**: Elements found in Spectrum 2*

Element	Atomic %
C	33.93
O	1.38
F	2.53
Si	0.23
P	0.39
S	23.76
Cr	0.39
Mn	23.80
Fe	13.58
Total:	100.00

Table 4-4 is the chemical analyze of Spectrum 1. The composition closely resembles that of Spectrum 2 with dominating elements once again being carbon, sulfur, and manganese. The exception is iron, which is very low in this area. Since the inclusion analyzed in Spectrum 1 is far bigger than the one in Spectrum 2 it is very likely that it also stretches deeper down in the matrix material. The possible shallowness of the inclusion in Spectrum 2 could explain why iron is so high in this sample.

***Table 4-4**: Elements found is Spectrum 1*

Element	Atomic %
C	34.67
O	1.68
F	2.64
Al	0.20
S	29.53
Mn	29.59
Fe	1.69
Total:	100.00

Given the data in Table 4-3 and Table 4-4 and the previous knowledge about the inclusions that occurs in the cast material at the Volvo factory in Skövde the inclusions seen here is most certainly composed of manganese sulfide.

The images in Figure 4-3 below shows the concentration of a number of elements found in the area displayed in Figure 4-2. Each element is characterized by a distinct color, e.g. red for carbon, green for copper etcetera.

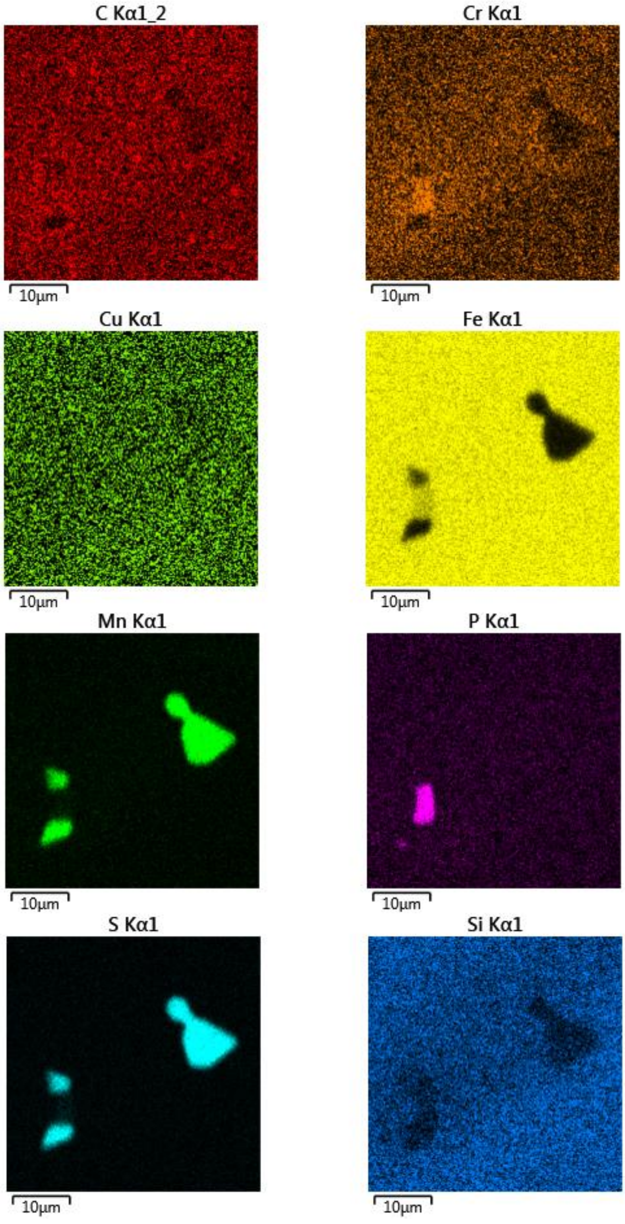

Figure 4-3*: Relative distribution of elements.*

4.2. Graphite structure

According to the ISO-standard 945-1, every material sample in the study had the graphite form I. The type of distribution was in most cases of type A. Other types of distribution found were type E and, in varying degree, type D.

4.2.1. Engine block 1

The graphite structure in block 1 can be seen in Figure 4-4. Both workpiece material samples that are displayed are taken from the surface material of the block, samples 1.2 from the top and 1.4 from the gable. Every sample except for sample 1.2 bottom and 1.4 top, shows a graphite form of type I and a distribution of type A. Some of the samples, especially 1.2 top and 1.4 top, has a more cloudy or blurred appearance of the graphite flakes. This is most likely due to imperfect polishing and are not signs of other types of graphite form or distribution. The classification of the samples are presented in Table 4-5.

Table 4-5: *Graphite structure of engine block 1.*

Sample	1.2 Top	1.2 Middle	1.2 Bottom	1.4 Top	1.4 Middle	1.4 Bottom
Form	I	I	I	I	I	I
Distribution	D	A	A	E	A	A

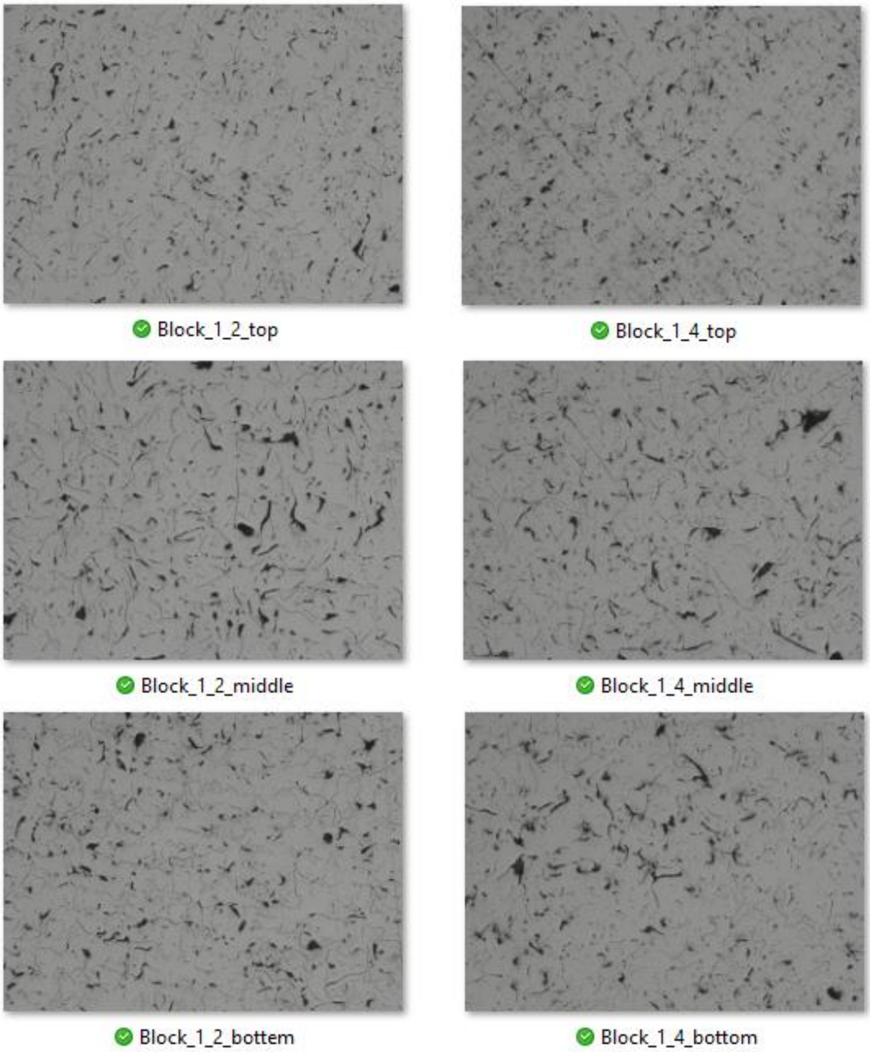

Figure 4-4: *Graphite structure of engine block 1, sample 2 and 4.*

A magnified image of sample 1.2 top can be seen in Figure 4-5 below. This sample has a graphite distribution of type E that is recognized by the tendency of the graphite flakes to orient in an ordered dendrite pattern. The cloudiness in the background is also apparent.

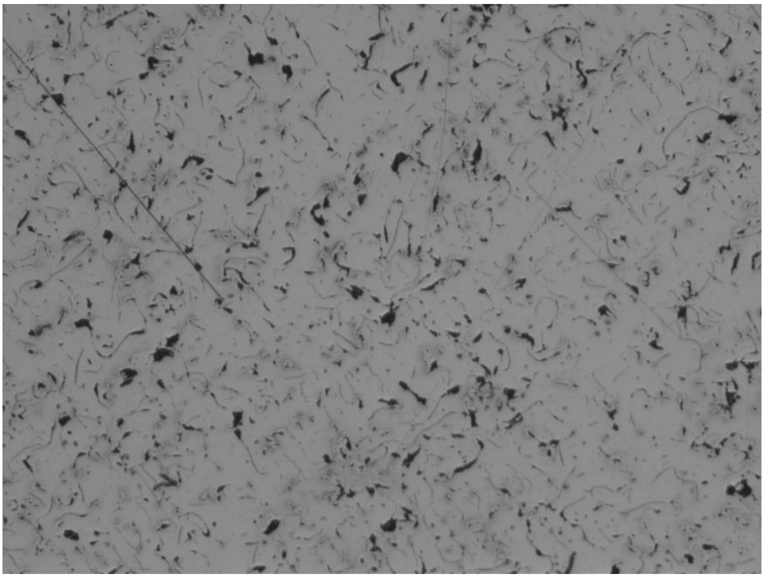

***Figure 4-5**: Graphite distribution of type E. The interdendritic graphite flakes which are characteristic for this kind of distribution is visible.*

4.2.2. Engine block 2

The graphite structure in block 2 is very uniform. Every sample, except 2.2 top, has a graphite form of type I and a distribution of type A. As in block 1 the samples has a cloudy and smeared out appearance which most likely is caused by imperfections during the polishing. Sample 2.2 has a graphite distribution of type A, but with some tendencies towards type D. The graphite structure can be seen in Figure 4-6 and the classification is presented in Table 4-6.

***Table 4-6**: Graphite structure of engine block 2. Sample 2.2 top has a distribution of type A with tendencies towards type D, this is indicated as A (D).*

Sample	2.2 Top	2.2 Middle	2.2 Bottom	2.4 Top	2.4 Middle	2.4 Bottom
Form	I	I	I	I	I	I
Distribution	A (D)	A	A	A	A	A

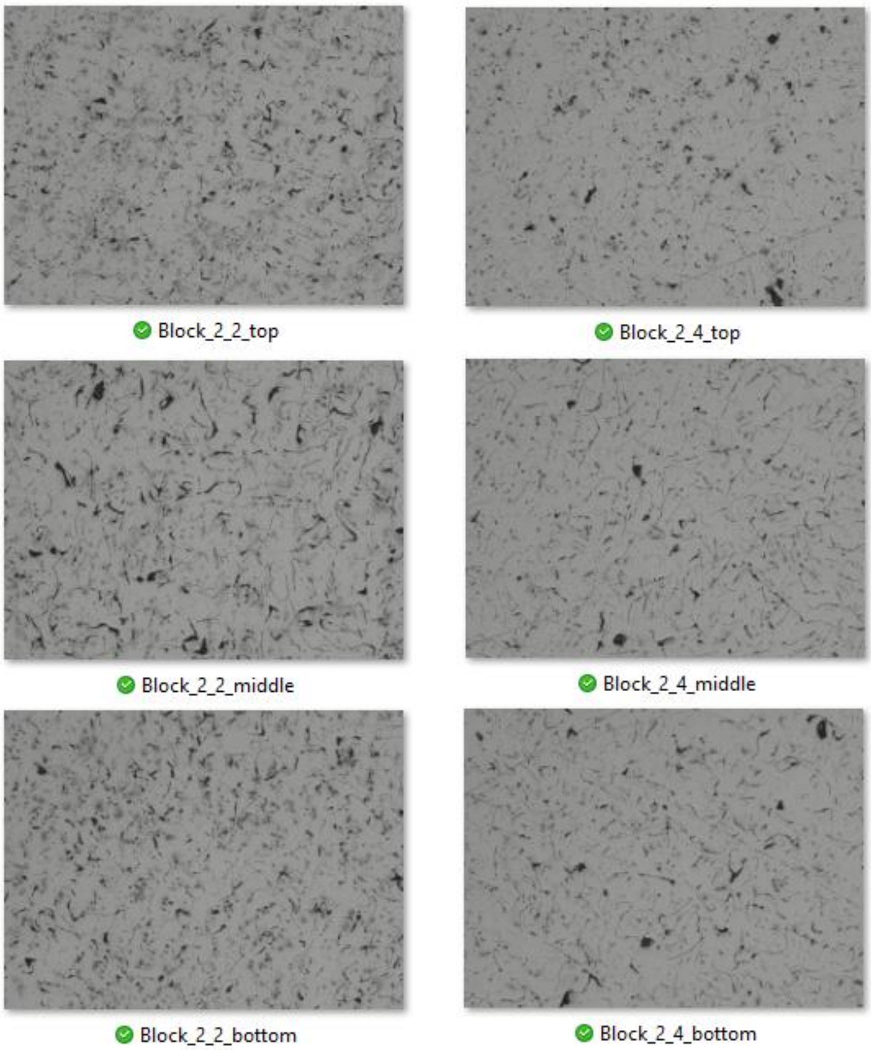

Figure 4-6*: Graphite structure of engine block 2.*

4.2.3. Engine block 3

The samples in block 3 was collected from the surface and from the bulk of the material and is shown in Figure 4-7 The formation found was of type I and the distribution of type E, A, or D. The classification of the graphite structure is presented in Table 4-7.

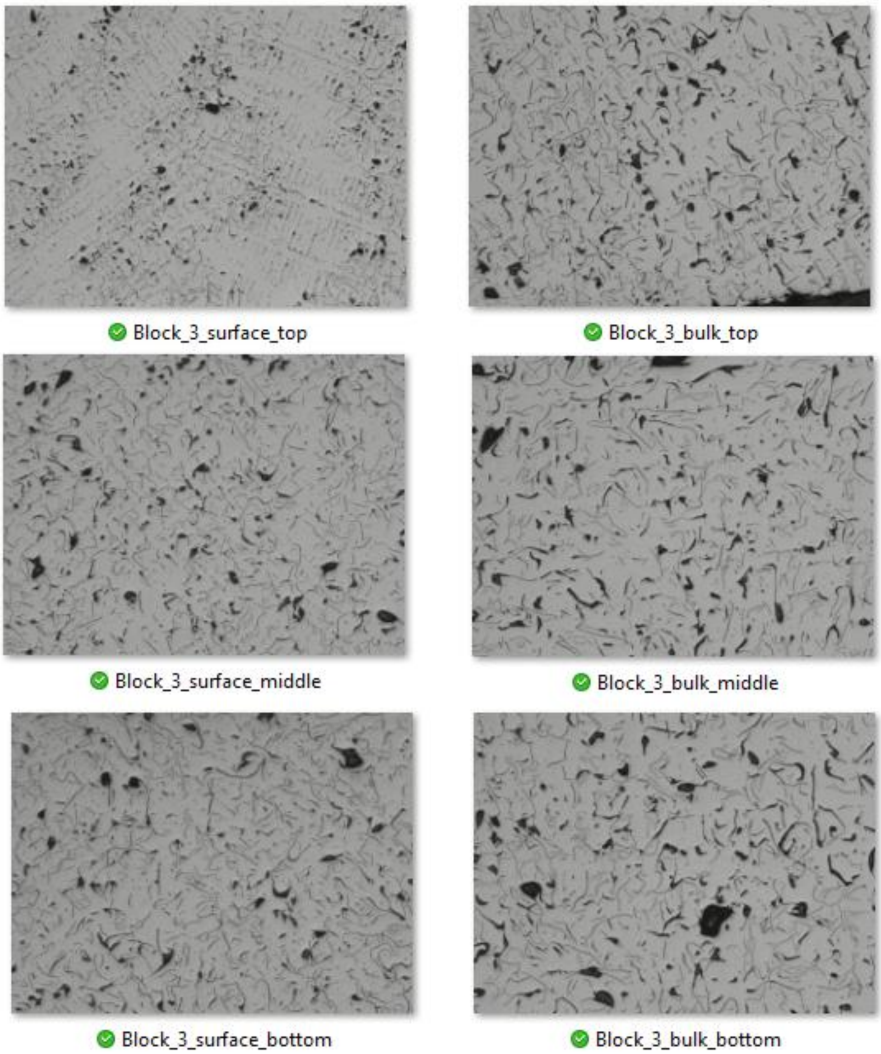

Figure 4-7*: Graphite structure of engine block 3.*

Table 4-7: *Graphite structure of engine block 3.*

Sample	3 surface top	3 surface middle	3 surface bottom	3 bulk top	3 bulk middle	3 bulk bottom
Form	I	I	I	I	I	I
Distribution	E	D	D	D	A	A

An enlarged image of the graphite distribution in the top area of the surface is shown in Figure 4-8. Here, the distribution type E is easily recognized by the characteristic square like pattern.

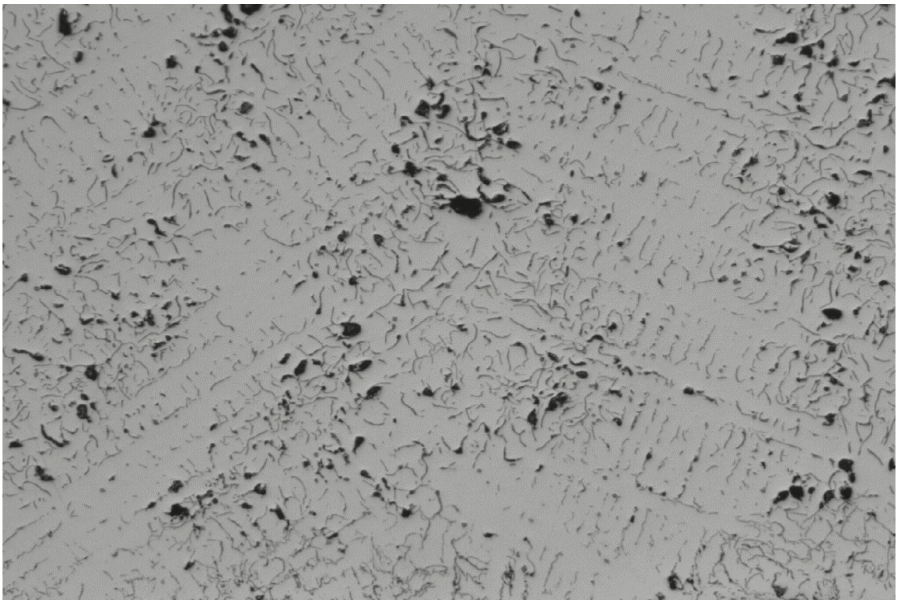

Figure 4-8: *Top area of the surface material in engine block 3. The distribution type E is easily recognized.*

Four of the samples have distribution type D. In Figure 4-9 the top area of the bulk can be seen, the distribution is of type D which can be recognized by the ordered pattern of graphite flakes.

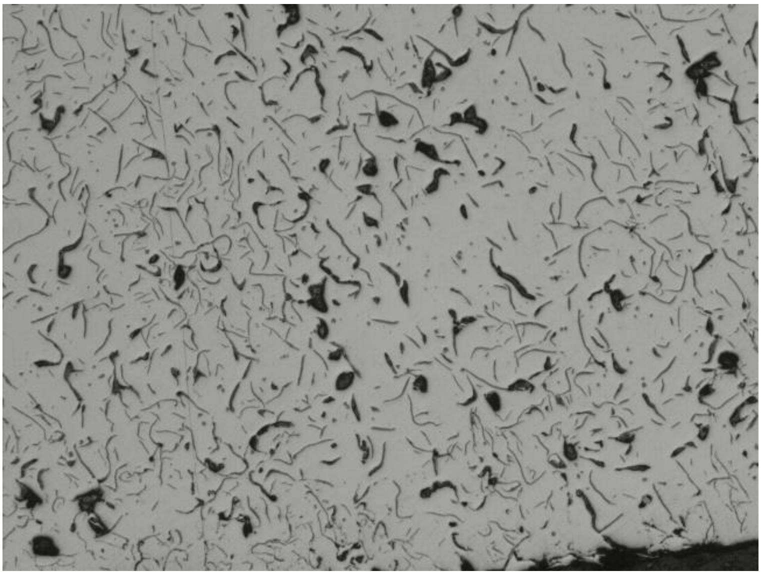

Figure 4-9: *Graphite structure of the top area in the bulk material of engine block 3. This sample have distribution type D, which is recognized by the way the graphite flakes are orientated.*

4.2.4. Engine block 4

In the surface material of engine block 4, distribution type A and E as well as type A with tendencies towards D is found. In the bulk material, the distribution found was only of type A. The graphite structure is shown in Figure 4-10 and the classification of the block 4 samples are presented in Table 4-8.

Table 4-8: *Graphite structure of engine block 4.*

Sample	4 Surface Top	4 Surface Middle	4 Surface Bottom	4 Bulk Top	4 Bulk Middle	4 Bulk Bottom
Form	I	I	I	I	I	I
Distribution	E	A (D)	A	A	A	A

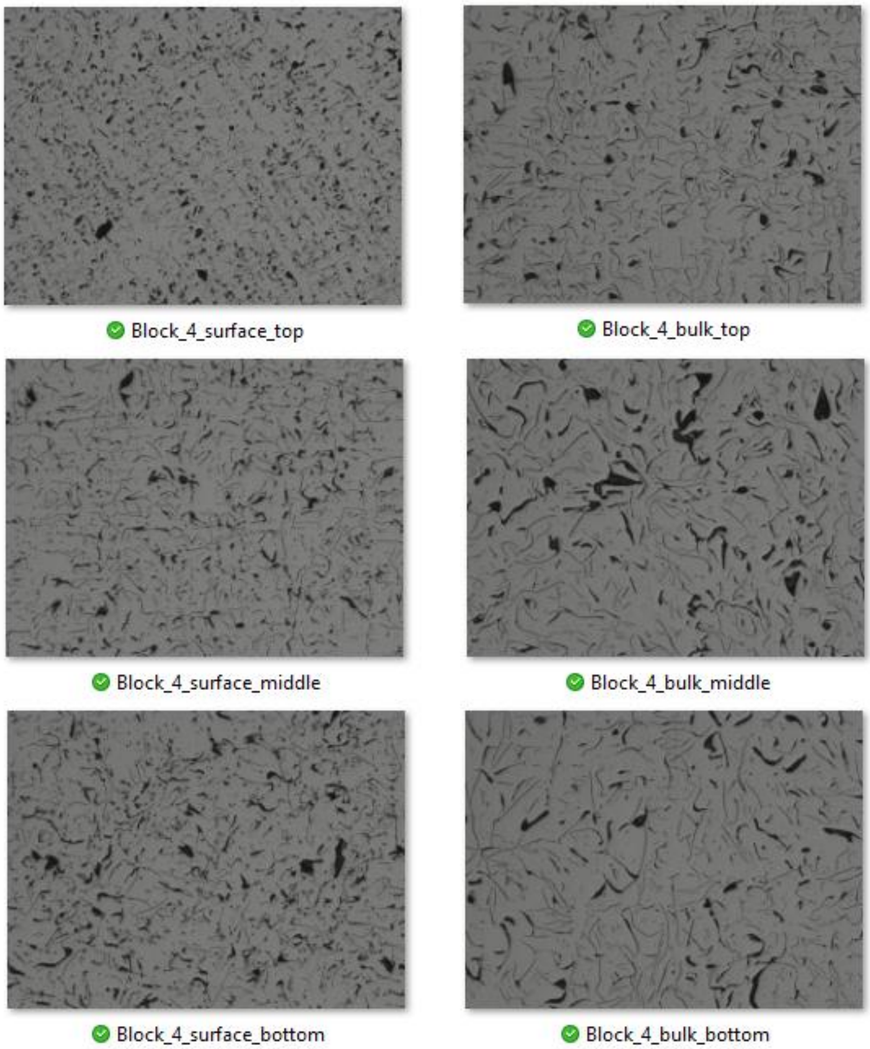

***Figure 4-10**: Graphite of structure of engine block 4.*

4.2.5. Engine block 5

There are only five workpiece material samples from block 5 instead of six samples as for the other blocks. One of the samples, from the middle area of the bulk material, was lost during handling and consequently there is no data obtained from this area.

The graphite structure of block 5 has a relatively high tendency to distribute the flakes in that of type D. One sample has however a clear distribution of type E. The graphite is shown in Figure 4-11 and the classification is presented in Table 4-9.

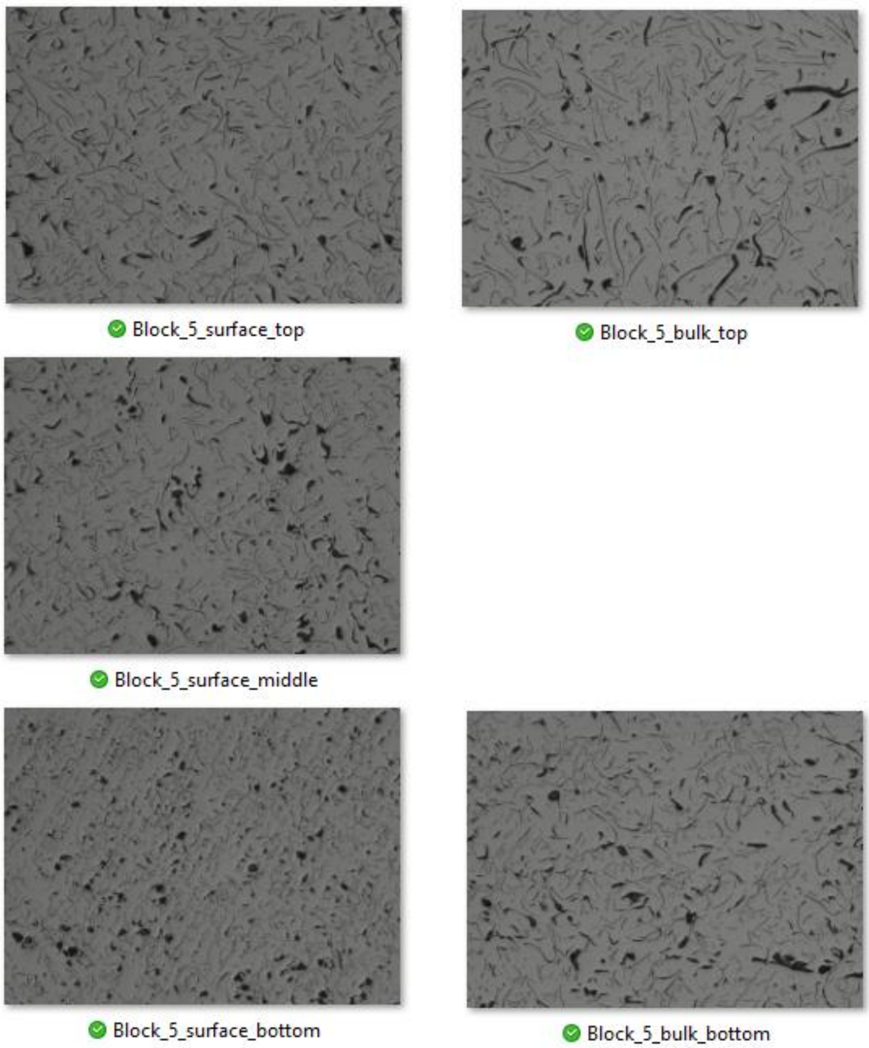

Figure 4-11: *Graphite structure of engine block 5.*

Table 4-9: *Graphite structure of engine block 5.*

Sample	5 Surface Top	5 Surface Middle	5 Surface Bottom	5 Bulk Top	5 Bulk Middle	5 Bulk Bottom
Form	I	I	I	I	I	I
Distribution	D	D	E	A	No data	A

The distinct type E distribution in the top area of the surface is shown in an enlarged version in Figure 4-12. The ribbon like orientation of the graphite flakes are easily distinguishable.

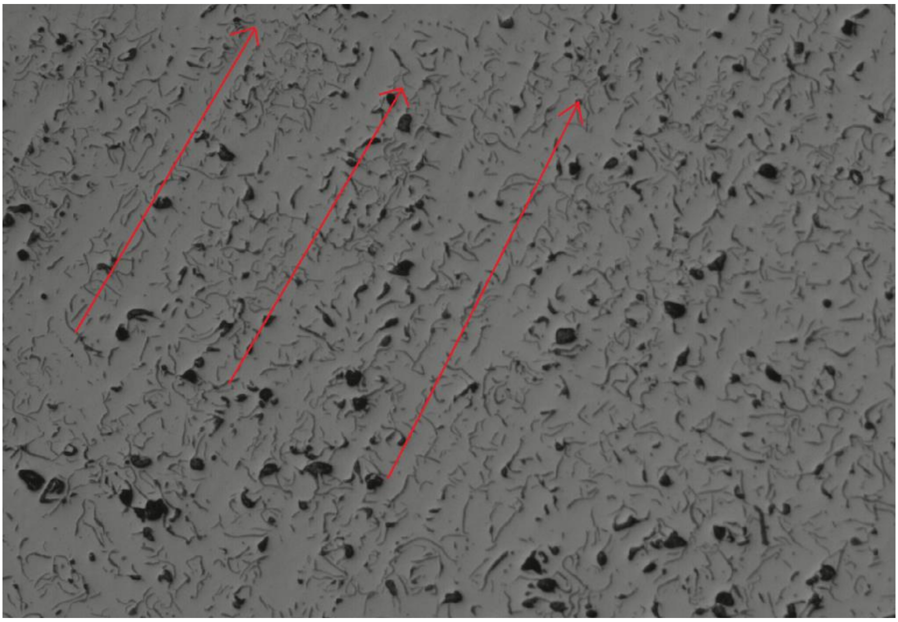

Figure 4-12: *The bottom area of the surface material sample. Notice the red arrows that indicates how the graphite flakes orientates themselves in a type E distribution.*

4.2.6. Summary of graphite structure and comparison between the engine blocks

A summary of the classification of the material samples are presented in Table 4-10. The results indicates that there are an unwanted variety between the engine blocks but also, to some extent, within the blocks.

***Table 4-10**: Classification of the graphite structure in the material samples*

Sample	1.2 Top	1.2 Middle	1.2 Bottom	1.4 Top	1.4 Middle	1.4 Bottom
Form	I	I	I	I	I	I
Distribution	D	A	A	E	A	A
Sample	2.2 Top	2.2 Middle	2.2 Bottom	2.4 Top	2.4 Middle	2.4 Bottom
Form	I	I	I	I	I	I
Distribution	A (D)	A	A	A	A	A
Sample	3 Surface Top	3 Surface Middle	3 Surface Bottom	3 Bulk Top	3 Bulk Middle	3 Bulk Bottom
Form	I	I	I	I	I	I
Distribution	E	D	D	D	A	A
Sample	4 Surface Top	4 Surface Middle	4 Surface Bottom	4 Bulk Top	4 Bulk Middle	4 Bulk Bottom
Form	I	I	I	I	I	I
Distribution	E	A (D)	A	A	A	A
Sample	5 Surface Top	5 Surface Middle	5 Surface Bottom	5 Bulk Top	5 Bulk Middle	5 Bulk Bottom
Form	I	I	I	I	No Data	I
Distribution	D	D	E	A	No data	A

Every examined material sample had the graphite form I. 16 out of 29 samples had graphite distribution of type A, the rest had E, D, or A with a tendency to D. The graphite distribution in the samples are presented in the diagram in Figure 4-13 and summarized in Table 4-11.

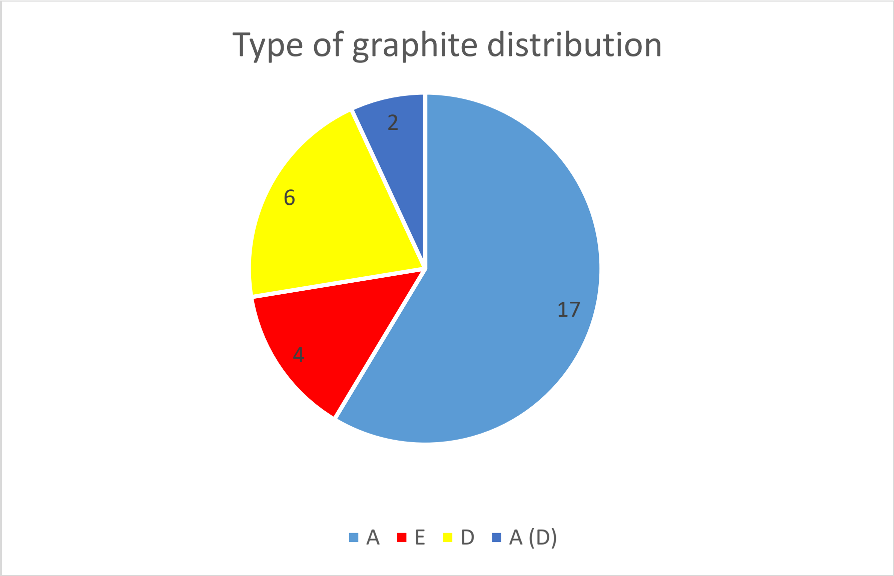

Figure 4-13: *Graphite distribution in the examined material samples. Type A is the most common.*

Table 4-11: *Prevalence of the different distribution types.*

Distribution	Prevalence
A	17
E	4
D	6
A, with a tendency to D	2

4.2.7. Variation between the samples

Three samples has the same graphite structure in the examined areas, one in block 1, one in block 4 and one in block 5. Most samples have one or more area where the distribution differs from the other samples. Table 4-12 below presents the homogeneity of the graphite structure of every sample together with a comment of the same.

***Table 4-12**: Number of divergent areas.*

Sample	Number of divergent areas	Comment
1.2	1	Top area has a graphite distribution of type D.
1.4	1	Top area has a graphite distribution of type E.
2.2	1	Top area has a graphite distribution of type A with tendencies towards D.
2.4	0	All areas has the same graphite structure.
3 surface	1	Top area has distribution type E.
3 bulk	1	Top area has distribution type D.
4 surface	3	All areas has different distribution
4 bulk	0	All areas has the same graphite distribution.
5 surface	1	Bottom area has distribution type E, the other areas has type D.
5 bulk	0	The two samples has the same graphite distribution.

The graphite distribution within the samples are divergent; only 3 out of 10 samples has the same distribution for every area. However, only one of the samples has different distribution in all areas.

4.2.8. Difference between bulk and surface material

There are difference in graphite structure between the surface material and the bulk material. As can be seen in Table 4-13, distribution type A occurs in all but one of the bulk material samples, whereas this type of distribution occurs in only about half of the surface samples.

***Table 4-13**: Graphite distribution in the surface and the bulk material.*

Graphite distribution	Surface (seven samples)	Bulk (three samples)
A	10	7
E	4	0
D	5	1
A+D	2	0

In engine block 3, 4 and 5, where both the surface and the bulk material was examined, the graphite distribution was even more divergent. Table presents the graphite distribution in the surface and the bulk material of these engine blocks.

***Table 4-14:** Graphite distribution in the surface and bulk material of engine block 3 to 5.*

Graphite distribution	Surface of engine block 3 to 5	Bulk of engine block 3 to 5
A	1	7
E	3	0
D	4	1
A+D	1	0

4.3. Chemical composition

The chemical composition of the material machined during the ten series are presented in tables and diagrams below. The exact composition is classified and each data point is therefore presented as percentage of the average value of all data points.

***Table 4-15**: Variation of oxide forming elements*

Oxide forming elements	Al	Si
series 1 block 1	99.52	99.68
series 2 block 2	105.18	99.27
series 3 no block	99.62	102.30
series 4 block 3	111.82	101.80
series 6 block 4	104.52	100.36
series 7 block 5	110.94	100.58
series 8 no block	89.71	99.44
series 9 no block	85.28	98.56
series 10 no block	88.68	97.96

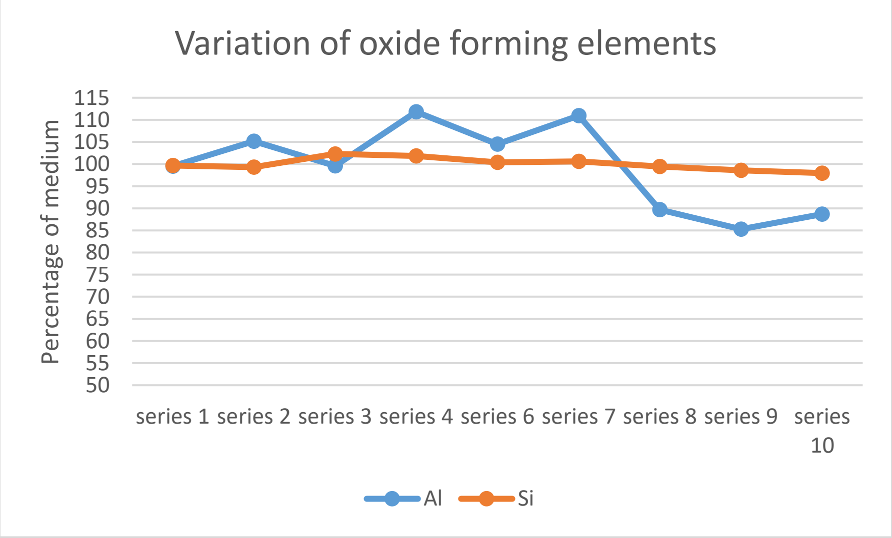

***Figure 4-14**: Variation of the oxide forming elements aluminum and silicon.*

Table 4-16: Variation of carbide forming elements.

Carbide forming elements	Cr	Mo	V	W	Ti	Ni
series 1 block 1	103.58	95.37	106.50	84.73	104.61	105.96
series 2 block 2	97.573	79.95	100.86	88.68	92.44	104.30
series 3 no block	98.34	80.92	92.80	63.15	112.87	104.96
series 4 block 3	99.78	74.65	95.80	97.89	110.47	98.89
series 6 block 4	102.22	114.65	129.61	103.42	115.24	104.77
series 7 block 5	104.21	104.38	99.48	70.00	84.36	92.89
series 8 no block	99.13	119.23	91.98	120.52	97.94	91.94
series 9 no block	104.05	114.29	92.93	138.42	96.24	97.10
series 10 no block	91.24	117.03	93.36	129.73	84.50	100.04

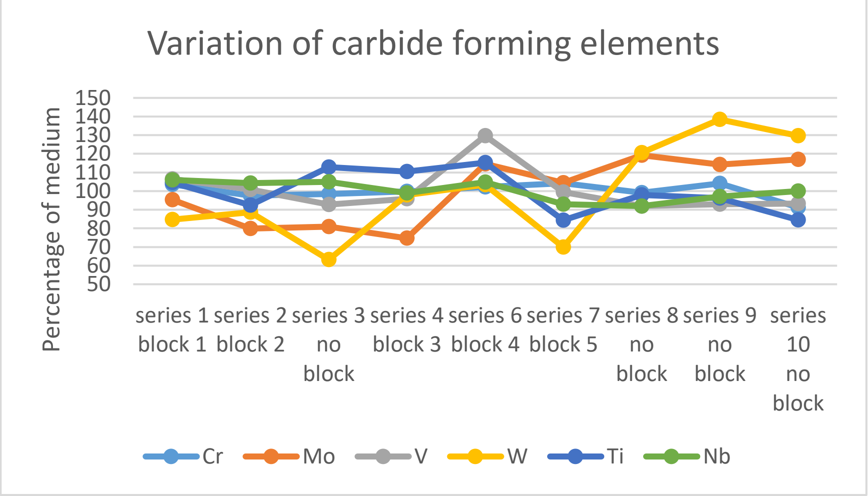

***Figure 4-15**: Variation of other forming elements.*

***Table 4-17**: Variation of other elements found in the workpiece material.*

Other elements	Mn	P	S	Cu	Sn
series 1 block 1	99.70	108.46	103.41	100.14	105.44
series 2 block 2	101.99	104.18	94.10	100.15	77.27
series 3 no block	103.45	96.36	96.14	100.20	91.04
series 4 block 3	103.39	95.46	106.92	101.03	104.12
series 6 block 4	103.39	89.22	99.73	100.75	113.22
series 7 block 5	96.67	95.77	101.83	101.25	77.84
series 8 no block	98.61	102.31	97.78	100.37	126.78
series 9 no block	93.87	104.05	100.60	99.06	124.09
series 10 no block	98.97	104.92	99.35	97.05	79.73

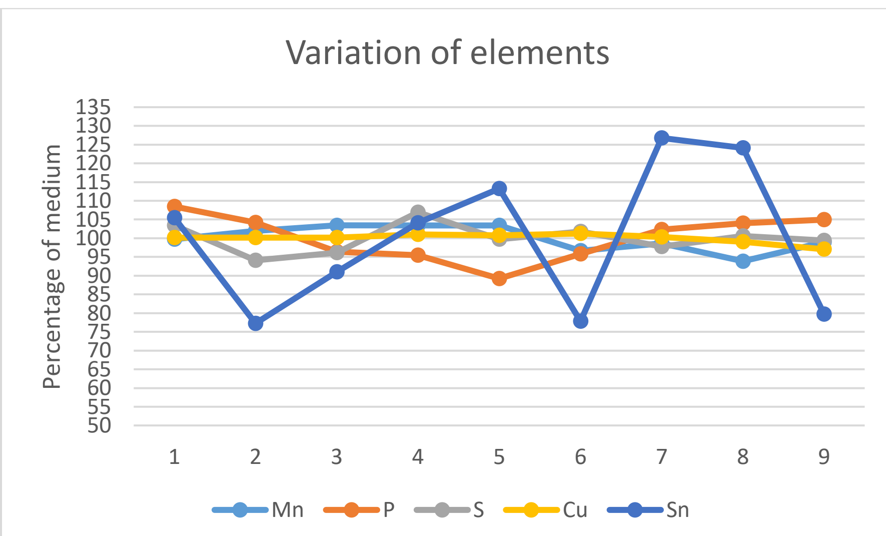

***Figure 4-16**: Variation of other elements found in the workpiece material.*

The carbon equivalent is of special interest and is therefore presented separate from the other elements in Table 4-18.

***Table 4-18**: Carbon equivalent for the data series.*

Sample	Carbon equivalent
Series 1, block 1	99.73
Series 2, block 2	99.86
Series 3, no block	100.53
Series 4, block 3	99.87
Series 6, block 4	98.28
Series 7, block 5	100.39
Series 8, no block	100.26
Series 9, no block	100.52
Series 10, no block	100.65

The carbon equivalent can also be seen in the line diagram in Figure 4-17.

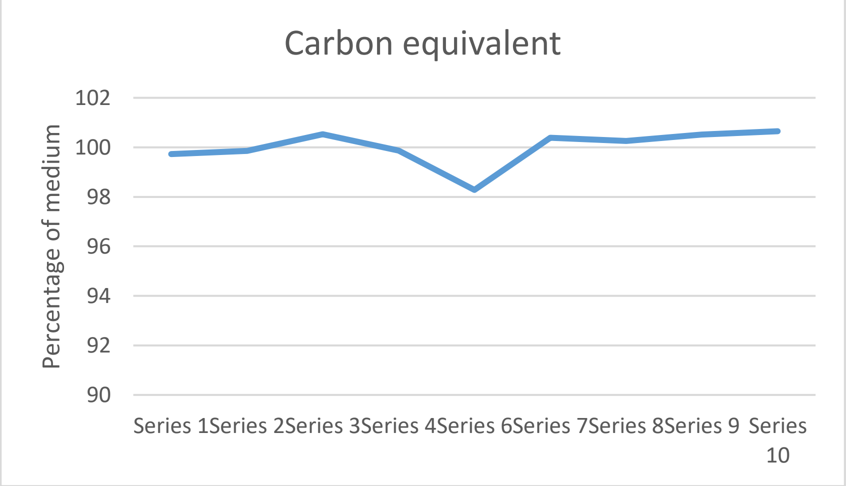

***Figure 4-17**: Content of carbon equivalent in the studied series as percentage if medium.*

4.4. Hardness

The hardness of the samples is presented in Table 4-19. The same samples whose graphite structure were examined were tested for hardness. In block 1 sample 1.2 was examined and in block 2 sample 2.2 was examined.

Table 4-19: *Brinell Hardness (HB) of the material samples.*

Sample	Block 1 surface	Block 2 surface	Block 3 surface	Block 3 bulk	Block 4 surface	Block 4 bulk	Block 5 surface	Block 5 bulk	Total mean value
Top	211	202	198	202	202	202	211	202	
Middle	202	202	202	198	195	195	207	202	
Bottom	202	195	202	198	195	187	215	202	
Mean value	205	199.7	200.7	199.3	197.3	194.7	211	202	201.2

In Figure 4-18 the HB of every data point is plotted. As can be seen the hardness is very consistent with only a few data points that deviates from the mean value. The highest value obtained was 215 HB, which was found in the surface of block 5. The lowest obtained value was 187 HB, which was found in the bulk material of block 4. This means that the difference between the highest and the lowest values obtained was 28 HB. The difference between the material sample with the highest average (the surface of block 5) and the sample with lowest average (the bulk of block 4) was 16.3 HB.

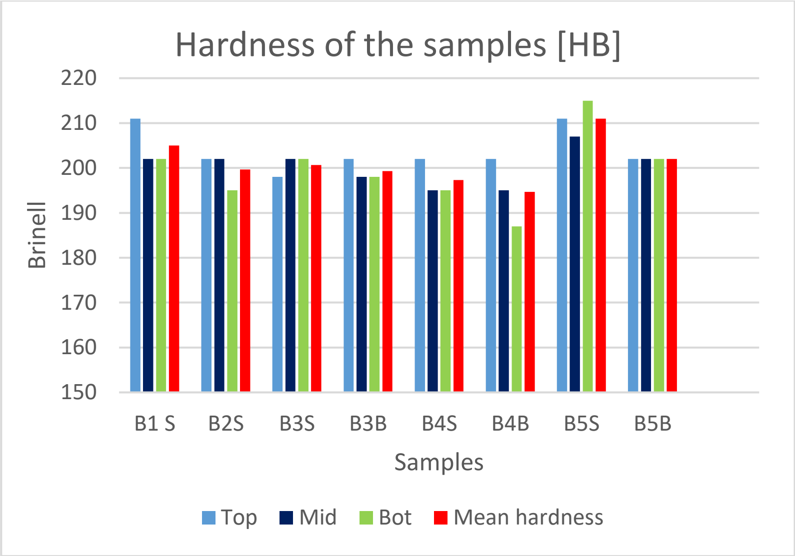

Figure 4-18*: Hardness of the workpiece material samples.*

Among the three samples where both the surface material and the bulk material was tested, the average hardness is slightly higher for the surface than for the bulk. Although this difference is only marginal in block 3 and 4, it is a bit more significant in block 5. The difference between the surface and the bulk samples is shown in Figure 4-19.

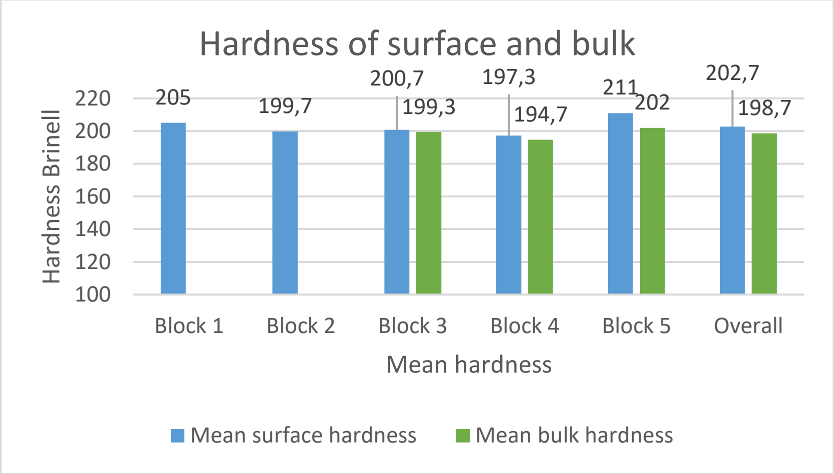

Figure 4-19*: Surface and bulk material hardness.*

4.5. Tool wear

The type of wear found on the cutting inserts were crater wear, thermal cracks, chipping, and in more serious cases, fracture. The crater wear took place at the rake side of the insert and an example this type a wear is shown in Figure 4-20 below.

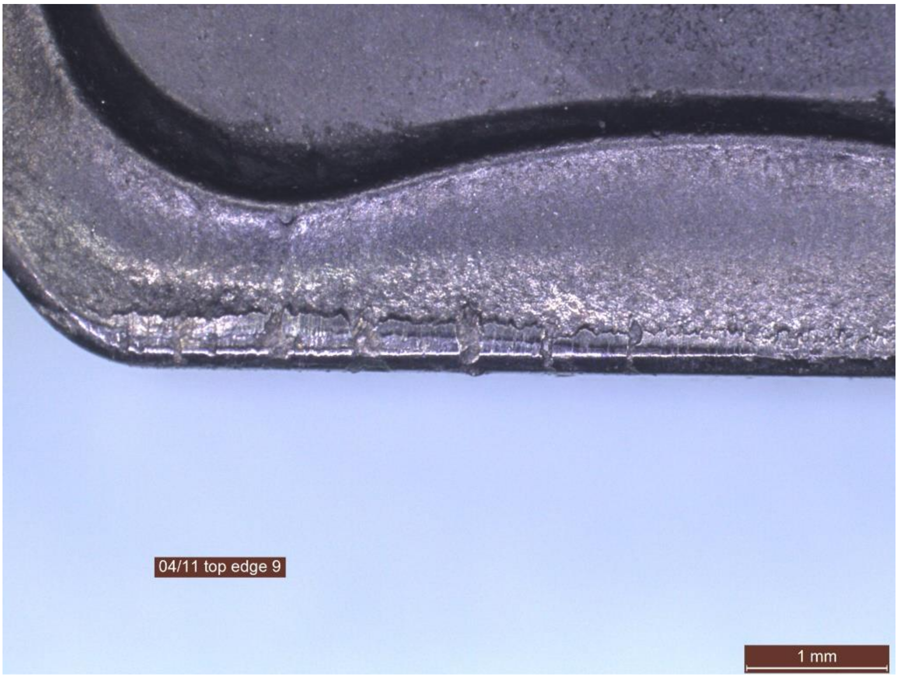

***Figure 4-20**: Crater wear on the rake side of the cutting insert.*

All of the examined cutting inserts had, in varying degree, crater wear of some sort. Thermal cracks were also always present in every insert. An example of initiated thermal cracks can be seen in Figure 4-21.

***Figure 4-21**: Initiated thermal cracks. Red arrows indicates the small, periodical notches typical for thermal cracks.*

The cutting tip of the insert in Figure 4-21 also had some visible wear, this was very typical of the wear pattern in the inserts and occurred in various degree in almost all of the inserts.

Some inserts show more serious form of fracture where parts of the cutting edge had been torn out. An insert with a severe fracture is shown in Figure 4-22.

Figure 4-22: *A cutting insert with a large chunk of edge torn out.*

4.5.1. Degree of wear

The degree of wear on the cutting tools in the 10 examined series are presented in Table 4-20 below. The table is color coded with red representing level 4, the highest degree of wear, yellow level 3, dark green level 2 and light green level 1, which is the lowest degree of wear. In series 1, only six cutting tool inserts were collected, in the other series 10 inserts out of 26 wear collected.

In series 1, 2, 4, 6, and 7 engine block were collected to enable an examination of the material that was machined by the inserts. Series with collected material samples are marked with a dark blue colour and series without are marked with light blue.

***Table 4-20**: The degree of wear on the examined cutting tools. Number 4 has the highest degree of wear and number 1 has the lowest. Which data series the blocks corresponds to is also included.*

Data Series	1	2	3	4	5	6	7	8	9	10
Material samples	Block 1	Block 2	No block	Block 3	No block	Block 4	Block 5	No block	No block	No block
CT1	2	3	4	2	3	1	2	1	3	3
CT2	2	1	3	4	4	4	1	1	2	3
CT3	3	2	3	4	4	2	1	2	3	3
CT4	1	2	1	3	2	2	2	2	2	1
CT5	3	2	1	4	2	3	2	2	2	1
CT6	3	3	2	4	2	3	2	2	1	4
CT7		1	1	3	1	3	3	1	3	1
CT8		1	1	4	2	4	1	1	1	4
CT9		4	1	4	2	4	3	3	1	3
CT10		2	2	4	2	3	2	1	1	4

A summary of the degree of wear is presented in Table 4-21.

***Table 4-21**: Summary of the degree of wear on the cutting inserts.*

Data Series		1	2	3	4	5	6	7	8	9	10
Degree of wear		Block 1	Block 2	No block	Block 3	No block	Block 4	Block 5	No block	No block	No block
Number of cutting inserts	1	1	3	5	0	1	1	3	5	5	3
	2	2	4	2	1	6	2	5	4	3	0
	3	3	2	2	3	1	4	2	1	2	4
	4	0	1	1	6	3	3	0	0	0	3

In Figure 4-23, the tool wear presented in Table 4-21 is illustrated. As can be seen in the diagram the degree of wear is highly varying from series to series. The by far most worn cutting tools was found in series 4 which was the series where the cutting tools needed to be replaced prematurely. Series 6 and 10 also displays a high degree of wear on the cutting tools whereas in series 7, 8 and 9 very little wear was found. Series 1, 2, 3, and 5 had a medium degree of wear on the cutting tools. Since only six tools were collected in series 1 the staple representing this series are adapted linearly to enable comparison with the other series.

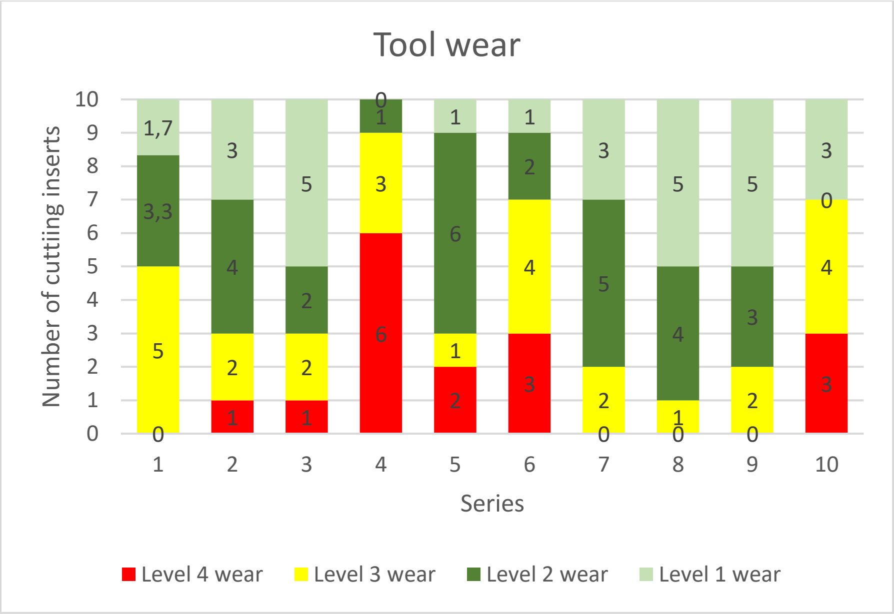

Figure 4-23*: Graphite illustration of the wear on the cutting inserts. Note that the values in series 1 are adapted to fit the number of tools collected in the other series.*

4.5.2. Comparison of tool wear between series

It is clear that there are differences in the amount of tool wear between the series. Series 4 has for example a considerably higher frequency of highly damaged tools than series 8. Table 4-22 below ranks the series according to the severeness of the tool wear found, wear ranking one being the most damaged tools and ranking 9 the least damaged. Comparison between series 1 and the other series are difficult to do since the number of examined cutting tools are 6 instead of 10. In this ranking, it was estimated that the degree of wear in series 1 was equal to that of series 3, hence they share the same position in the ranking.

__Table 4-22__: Data series ranking according to the severeness of the tool wear.

Series	Wear ranking	Wear ranking	Series
1	6	1	4
2	5	2	6
3	6	3	10
4	1	4	5
5	4	5	2
6	2	6	1
7	7	6	3
8	9	7	7
9	8	8	9
10	3	9	8

4.5.3. Distribution of tool wear

The wear on the cutting tool inserts were fairly even distributed between the four levels. The most common type of wear was level 4 with 30 % of the cutting tool inserts categorized in this group. The least common type of wear was level 4 with 17 % of the inserts. A summary of the distribution of wear levels can be seen in Figure 4-24.

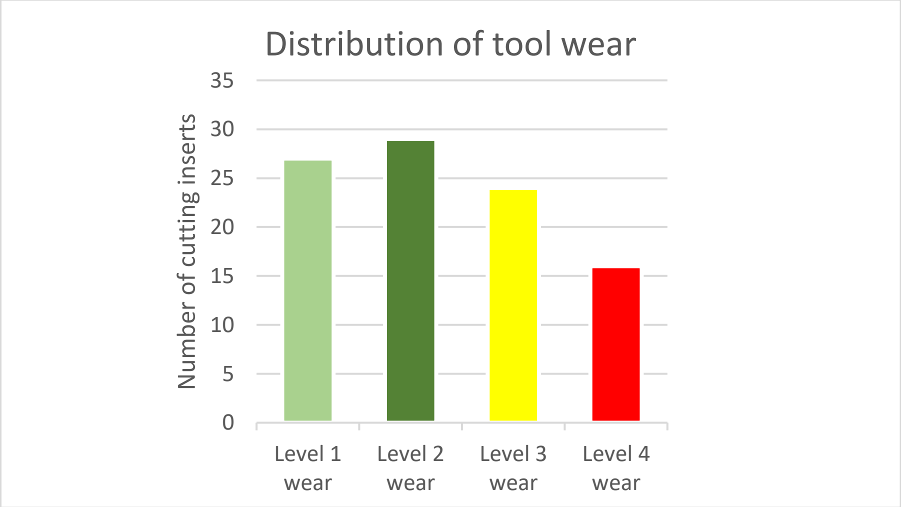

__Figure 4-24__: Distribution of tool wear.

4.6. Inclusions

The number of Ti(C,N) inclusions in the examined areas of the material samples are listed in Table 4-23.

***Table 4-23:** Number and type of Ti(C,N) inclusions in the examined area of the material samples.*

Type of inclusion	Block 1 surface	Block 2 surface	Block 3 surface	Block 3 bulk	Block 4 surface	Block 4 bulk	Block 5 surface	Block 5 bulk
Large detached	3	4	7	4	3	8	1	5
Large nucleated	4	5	5	2	3	6	3	5
Medium detached	20	19	40	22	19	18	13	19
Medium nucleated	7	6	11	12	12	10	7	5
Small detached	15	24	30	31	23	26	27	23
Small nucleated	6	4	10	2	7	7	7	8
Detached total	38	47	77	57	45	52	41	47
Nucleated total	17	15	26	16	22	23	17	18
Total	55	62	103	73	67	75	58	65

The data in Table 4-23 is presented in graphical form in Figure 4-25.

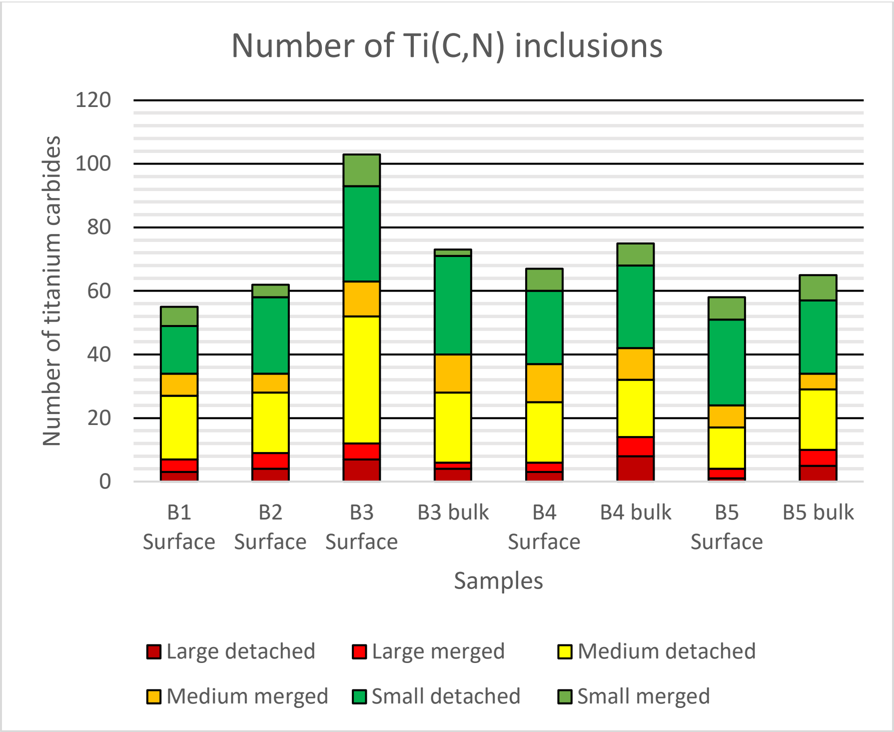

***Figure 4-25**: Number and type of Ti(C,N) inclusions in the examined material.*

As can be seen in the diagram, the number of Ti(C,N)-inclusions vary significant between the samples. The surface of block 3 is the sample that, by far, had the highest concentration of inclusions. The concentration of inclusions in the surface of block 3 was almost the double that of the surface of block 1 who was the sample with the lowest concentration. The proportion of large, medium and small inclusions are fairly consistent between the samples. That is, if a sample has a high concentration of large inclusions it will also have a high concentration of small inclusions. The same can be said of the concentration of Ti(C,N) inclusions nucleated to manganese sulfide inclusions in relation to detached Ti(C,N) inclusions. If a sample has a high concentration of nucleated inclusion it will also have a high concentration of detached inclusions.

4.6.1. Prevalence of the different types of inclusions

The overall distribution between the six categories of inclusions is presented in the circular diagram in Figure 4-26.

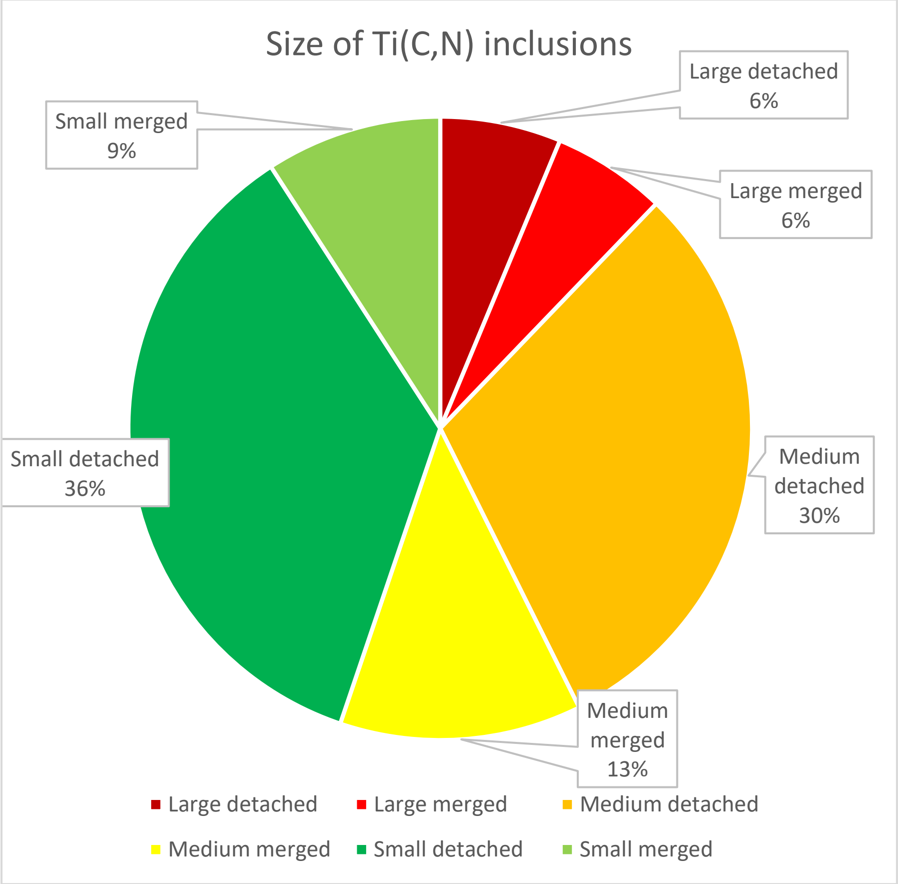

Figure 4-26*: Overall distribution of size and type of Ti(C,N) inclusions. Green colour scale represents small sized inclusions, yellow medium sized and red large sized.*

Small and medium sized inclusions makes up for 88 % of the number of inclusions found. Small inclusions are 45 % of the total and medium sized 43 %. Only 12 % of the inclusions are large. In all samples with the exception of the surface of block 3 and the surface of block 1 small inclusions are more common than medium sized ones. Large inclusions are in every sample less common than small and medium sized.

In total, 28 % of all inclusions found were nucleated with a manganese sulfide inclusion and 72 % were detached. Nucleated inclusions becomes more common the larger the inclusions gets. Among large inclusions the share of nucleated inclusions are 50 %. Medium sized inclusions are nucleated 29 % of the cases and among small inclusions only 20 % is nucleated.

4.6.2. Difference between surface and bulk material

There are overall little differences between the concentration of Ti(C,N)-inclusions in the surface and the bulk material. The total number of inclusion found in the three surface samples and the three bulk samples are shown in Figure 4-27.

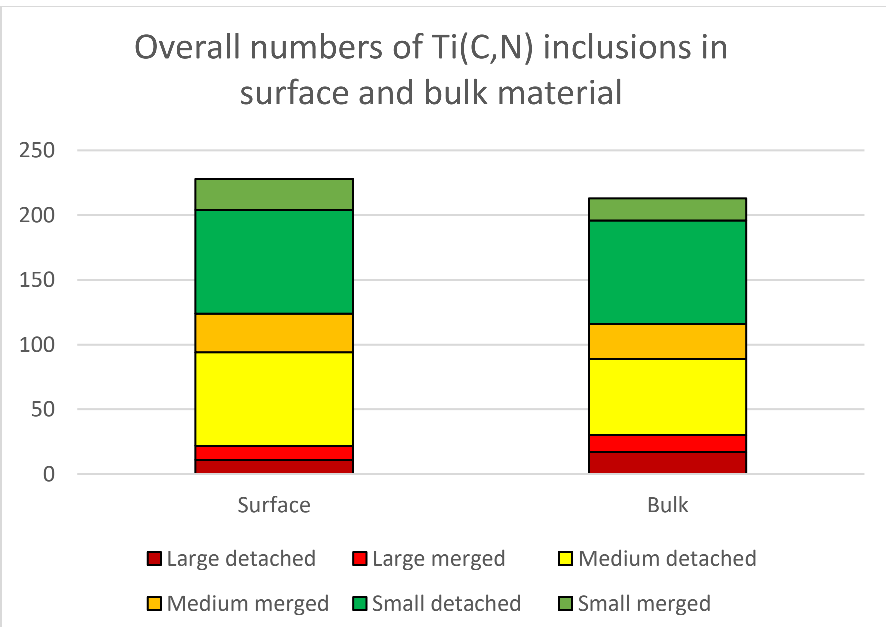

***Figure 4-27**: Total number of Ti(C,N) inclusions found in the surface and bulk material in block 3, 4, and 5.*

As can be seen there are slightly more inclusions found in the surface than in the bulk material. However, in two out of three blocks, block 4 and 5, there are more inclusions in the bulk than in the surface, although the difference is not very significant. In block 3, there is considerably more inclusions found in the surface. The surface sample of block 5 is also the sample who has by far the highest concentration of inclusions. This very high concentration is the sole reason why the overall number of inclusions is higher in the surface than in the bulk. The total number of inclusions found in the surface and the bulk material in block 3, 4, and 5 are presented in Table 4-24.

Table 4-24*: Number of Ti(C,N) inclusions in the surface and bulk material.*

Type of inclusion	Surface	Bulk
Large detached	11	17
Large nucleated	11	13
Medium detached	72	59
Medium nucleated	30	27
Small detached	80	80
Small nucleated	24	17
Total	228	213

4.6.3. Comparison of inclusions between series

The concentration of Ti(C,N) inclusions in the surface material is highest in block 3. Second highest is found in block 4. Block 1 and 2 have nearly identical concentration of large and medium inclusions, block 2 however has more small inclusions than block 1. Hence, block 2 has the third highest concentration and block 1 the fourth highest. Block 5 has the lowest concentration of all blocks if only the medium and large inclusions are taken into account, the total number of inclusions are however slightly higher than for block 1. Since the difference in total number of inclusions are only marginally higher for block 5 than for block 4, but significant lower in medium and large ones, block 5 is ranked lower than block 4. Figure 4-28 displays a diagram of the concentration of inclusions in the surface material ranked from highest to lowest.

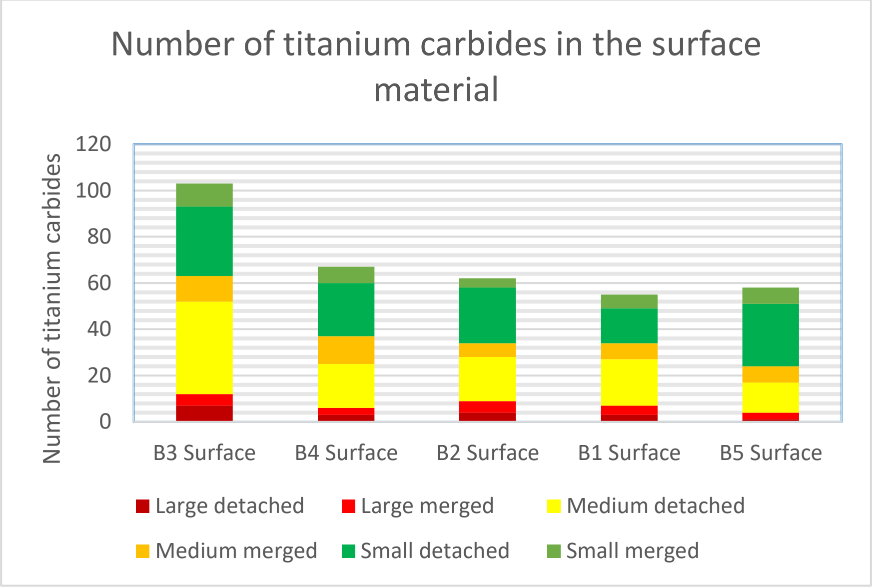

***Figure 4-28**: Number of inclusions in the surface material.*

The ranking of the blocks by concentration of inclusions are presented in Table 4-25 below. Position 1 is the highest concentration and position 5 the lowest.

***Table 4-25**: Ranking of the engine block according to the concentration of Ti(C,N) inclusions.*

Block	Concentration of titanium carbides	Concentration of titanium carbides
1	Highest	Highest
2	Second highest	Second highest
3	Middle	Middle
4	Second lowest	Second lowest
5	Lowest	Lowest

4.6.4. Shape of Ti(C,N) inclusions

In almost all of the cases, the inclusions have sharp edges and forms in a rectangular shape, although exceptions from this are not unusual. In Figure 4-29, an example of a large, rectangular shaped inclusion with sharp edges can be seen.

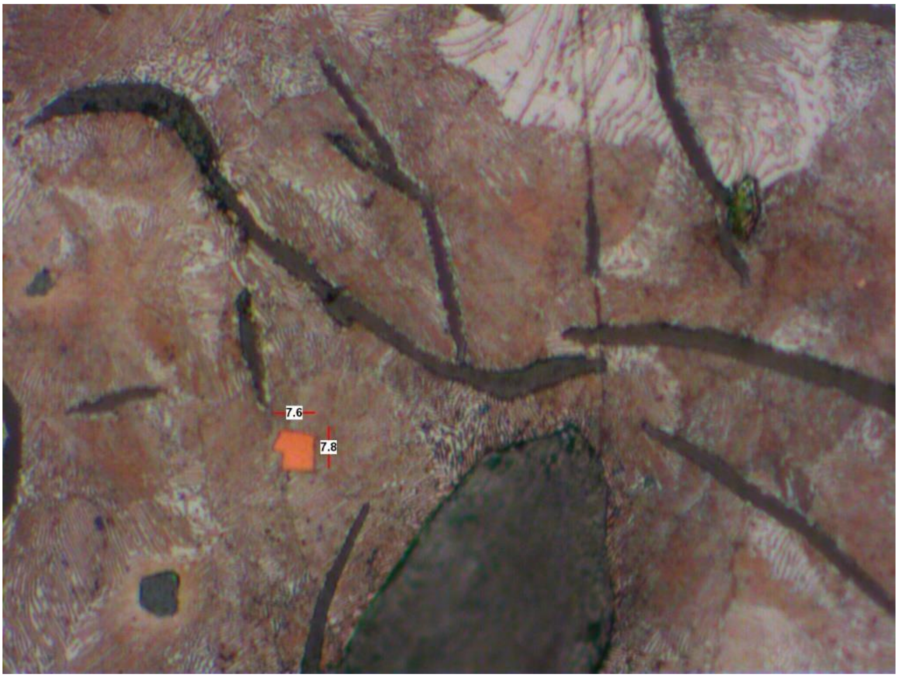

Figure 4-29*:The orange square shaped object is a large Ti(C,N)-inclusion with sharp edges. The curved strings are graphite flakes and the large black object in the lower middle is a manganese sulfide inclusion*

A more rounded appearance of inclusions can be seen in Figure 4-30 were two clusters of small sized inclusions are displayed.

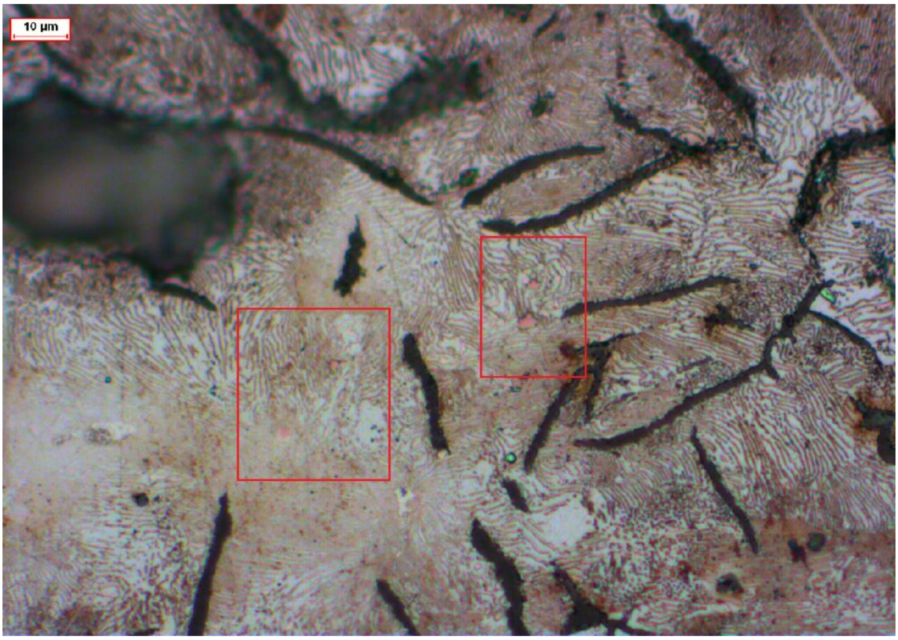

***Figure 4-30**: Red squares indicates areas with small, orange Ti(C,N)-inclusions with rounded edges.*

4.6.5. Shape of nucleated inclusions

Ti(C,N) inclusions that are nucleated to manganese sulfide inclusions are in most cases attached to a manganese sulfide. An example of this can be seen in Figure 4-31.

Figure 4-31*: In the middle of the image, a Ti(C,N)-inclusion nucleated to a manganese sulfide.*

In some cases, the Ti(C,N) inclusion completely surrounds the manganese sulfide, thus creating a large surface of inclusion for the cutting tool to work through. In Figure 4-31 an example of such an inclusion can be seen.

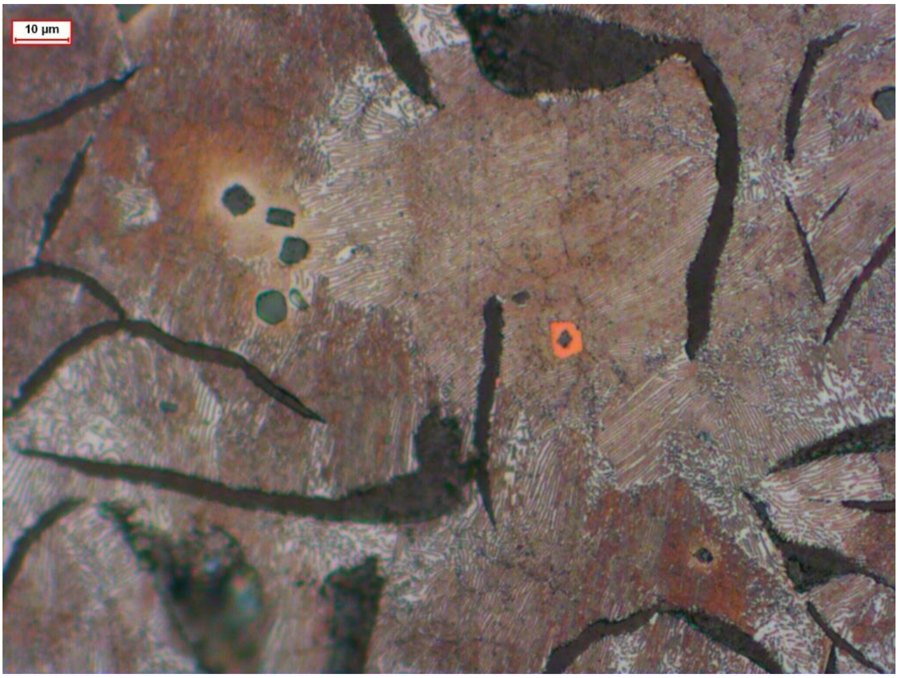

Figure 4-32*: In the middle, an example of a Ti(C,N)-inclusion that completely surrounds a manganese sulfide.*

5. Discussion

This chapter discusses the results of this study and interprets the consequences the variation of material properties has on tool wear and machinability. Theories presented in Chapter 2 are used to explain correlations between material properties and evaluate the validity of the results.

5.1. Composition of inclusions

The results of the SEM-XEDS analysis clearly indicates that the vast majority of the inclusions observable in the workpiece material were either manganese sulfides or titanium carbonitride Ti(C,N). The XEDS has a tendency to overrate lighter elements such as carbon and nitrogen, which could explain why the results indicates the presence of other elements than manganese, sulfur, nitride or titanium. The underlying material also influences the XEDS analysis caused by the selected accelerating voltage, i.e. it does not measure only the visible material on the surface, but also the material in the excitation volume, which could explains the relatively high levels of other elements than those found in the inclusions.

5.1.1. Size morphology and distribution

The Ti(C,N) inclusions tends to be rectangular in shape and to have sharp edges. Small inclusions are less often nucleated with manganese sulfides than large ones. Half of the large inclusions are nucleated with a manganese sulfide compared to only 20 % of the small ones. Medium sized titanium carbides are nucleated in 29 % of the cases.

5.1.2. Concentration of Ti(C,N) inclusions

There are a significant variation in the concentration of Ti(C,N) inclusions found in the workpiece material. The number of Ti(C,N) inclusions found in the examined areas ranges from 55 up to 103.

The method used to find and estimate the concentration of Ti(C,N) inclusions have some flaws, it is for example possible that some inclusions could have been missed during the counting. This is especially true for the smaller sized inclusions given the human factor in the ocular examination used as method. However, every sample shows approximately the same relationships between the number of large and medium or small inclusions. That is, if a material sample has a high concentration of large inclusion, it also has a large concentration of small inclusions and vice versa. This implies that the relative concentration of inclusions is still the same between the sample even if some of the small inclusions have been missed. This is so because it is highly unlikely that a large inclusion have been missed since they are so easy to spot.

5.1.3. Concentration of inclusions in bulk and surface material

Since the entire material sample could not be examined, it is possible that the area that were examined were not representable for the sample as whole. This objection is in part contradicted by the fact that the bulk and the surface material in block 3, 4, and 5 have a concentration of inclusions that are comparable to each other. The exception is the surface of block 3 where the surface area shows the highest concentration of all samples and considerably higher than the bulk of block 3. However, the concentration is the third highest in the bulk of block 3 so it is reasonable to assume that even if the examined surface area by chance would be higher than in the rest of the sample it would still be a very high concentration in the sample as whole.

Overall, there seems to be no greater difference between the concentration of inclusions in the bulk and surface material. However, the number of comparable samples are too low to draw any certain conclusion other than one area tends to have a high concentration if the other one also has a high concentration and vice versa.

5.2. Graphite structure and Hardness

The form of the graphite in all of the workpiece material samples were of type I. The distribution varied between A, D and E. There were clear differences between the engine blocks but also within the blocks. Most notably however is the difference between the bulk and the surface material, with only one exception the graphite distribution found in the bulk material was of type A. The surface cools quicker than the bulk, and since type D and E is associated with a more rapid cooling of the melt compared to type A. Hence, it is possible that a difference in cooling time is the explanation to the difference in graphite distribution between the bulk and the surface material.

5.2.1. Correlation between graphite structure and hardness

Table 5-1 presents the hardness and graphite distribution types of the workpiece material. There are some differences in the mean hardness of the different distribution types. Type A has the lowest mean hardness with 199.2 HB. The highest mean HB is for type E with 204. The overall mean HB is 201. This result is in line with what is presented in the theory section since graphite distribution of type D and E is often harder than the softer type A.

Table 5-1: *Hardness of the material by different types of graphite distributions.*

A [HB]	A (D) [HB]	D [HB]	E [HB]
202	202	211	198
202	195	202	202
202		202	215
195		202	
198		211	
198		207	
187			
202			
195			
187			
202			
202			
Mean hardness [HB]	Mean hardness [HB]	Mean hardness [HB]	Mean hardness [HB]
197.7	198.5	205.8	205.0

As can be seen in Table 5-1 there are more differences within the distribution types than between them. Type E has the most divergent hardness. One sample was measured to 215 HB which is well the highest measured hardness of all samples. However, one sample had 198 HB, making type E the graphite distribution with the highest spread.

The hardness in distribution type D is similar to typ E in hardness, both having a higher than average hardness. The data points are however not as spread out as or the other types. Distribution type A, with tendency to D has more in common with type A than D when it comes to hardness. However, the samples with this kind of distribution are very few so no clear trend can be seen.

Distribution type A, which is the by far most common type, has the lowest mean hardness of 197.7 HB. Most samples have a HB of 202 or 198, and no sample exceed 202 HB, making it a uniformly soft distribution type.

5.2.2. Hardness and inclusions

In general, material samples with a low concentration of inclusions tends to be harder than those with a high concentration of inclusions. In Table 5-2, the samples in the left column are ordered according to concentration of inclusions, from highest to lowest. In the right column, the samples are ordered according to the hardness, from softest to hardest. Every sample has the same color code in both columns. The color code visualize the correlation between hardness and concentration of inclusions. The material sample from the surface of engine block 3 had an exceptionally high concentration of inclusion but has only medium hardness. All other samples tends to have a higher hardness if the concentration of inclusions are low and vice versa.

***Table 5-2**: Engine block ordered after concentration of inclusion and hardness. The engine blocks have the same color code regardless of column in the table.*

Material samples, ordered from highest concentration of inclusions to lowest	Material samples, ordered from softest to hardest
Block 3 surface	Bock 4 bulk
Block 4 bulk	Block 4 surface
Block 3 bulk	Block 3 bulk
Block 4 surface	Block 2 surface
Block 5 bulk	Block 3 surface
Block 2 surface	Block 5 bulk
Block 5 surface	Block 1 surface
Block 1 surface	Block 5 surface

This correlation is, although somewhat contra-intuitive since the inclusions are so hard, in line with what previous studies of the subject suggests [18] [19]. The inclusions could be acting as fracture initiator or in other ways weaken the metal matrix of the material. However, since there are few samples and the correlation is only general in most cases and non-existing in one case it is possible that there are other factors that could be the explanation to the tendency of high hardness for samples with low inclusion concentration.

5.3. Chemical composition

There are considerable difficulties in finding a correlation between the machinability of the grey cast iron and the chemical composition of the examined material in the engine blocks. The biggest problem is the relative scarcity of data. There are only data from five engine blocks and the number of elements that are detected in the chemical analysis amounts to 14. With this high number of variables and low number of data series, any far-reaching conclusions should not be drawn. It should also be noted that the data of the chemical content is the average of a whole series of machined engine blocks. Individual engine blocks in a series could therefore differ significantly from the numbers presented in this chapter.

Some elements vary, percentage wise, a lot from one series to another, while some are about the same in every series. Generally, there are a higher variation between the samples in those elements that are trace elements, like titanium or tungsten, than for alloying elements such as chromium.

5.3.1. Chemical composition and inclusions

Titanium is of special interest since this is crucial in forming titanium carbide, one of the main focuses of this study. The variation of titanium between the blocks can be seen in Figure 5-1.

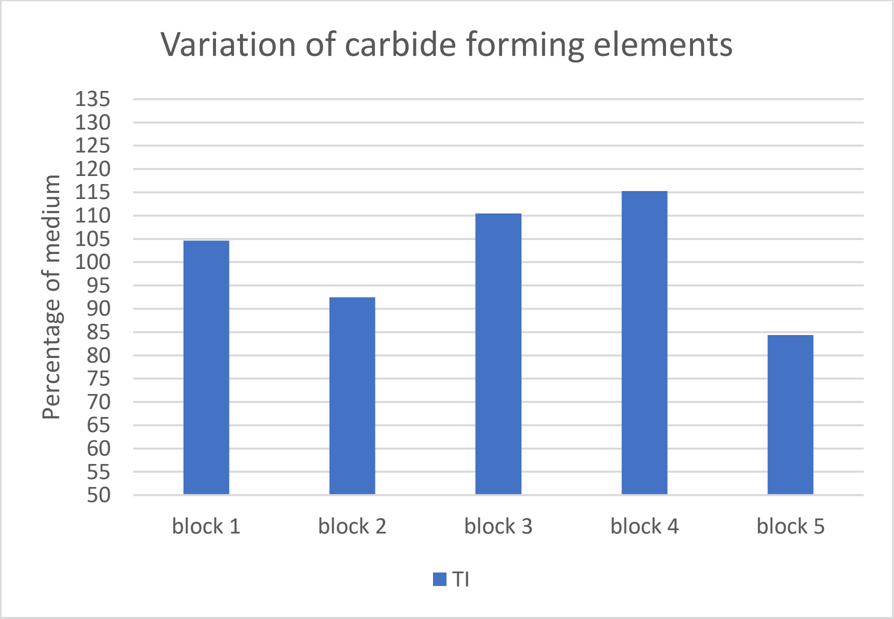

Figure 5-1: *Relative titanium content in block 1 to 5.*

There is a substantial variation in the amount of titanium found in the engine blocks and this will according to the theory have an impact on the concentration of titanium carbides in the blocks. In Table 5-3 the concentration of titanium carbides and the titanium content in the material is compered. As can be seen there are a general, but not absolute, correlation between the amount of titanium in the material and the concentration of Ti(C,N)-inclusions. Block 3 that has the highest concentration of Ti(C,N)-inclusions has the second highest titanium content. On the other end of the scale, block 5 has both the lowest concentration of Ti(C,N)-inclusions and the lowest titanium content. The data in Table 5-3 thus confirms that the titanium content has an impact of the concentration of Ti(C,N)-inclusions.

Table 5-3: *Concentration of titanium carbides compared to the titanium content of the workpiece material.*

Engine block	Concentration of titanium carbonitrides	Titanium content
3	Highest	Second highest
4	Second highest	Highest
2	Middle	Second lowest
1	Second lowest	Middle
5	Lowest	Lowest

How the other carbide forming elements affects the concentration of other types of inclusions or the overall machinability of the material is impossible to say from this data. Block 4, which has the second most tool wear, has an unusually high content of a number of carbide forming elements. Out of the six elements measured, it has the highest content in four of them and the second highest in one. This would suggest that the content of carbide forming elements have an impact of the machinability of the material. However, Block 3, which had the most severe tool wear, do not have a particularly high content of carbide forming elements, except for titanium. In fact, it only has a higher than average content of these elements in two cases, which is tungsten and as previously mentioned, titanium. However, tungsten is the least common element out of the 14 measured and it is doubtful that it affects the machinability at all.

5.3.2. Carbon equivalent and graphite structure

The carbon equivalent is the chemical factor that has the lowest variation. In engine block 1 to 3 the carbon equivalent is almost exactly the same. In engine block 4 the carbon equivalent is about 1.5 percentage lower than these blocks and engine block 5 about 0.6 percentage higher. These small differences in carbon equivalent content could therefore not be the explanation to the differences in graphite structure.

5.4. Tool wear

There were three main types of tool wear found on the inserts. Crater wear, thermal cracks, and fracture. All inserts showed crater wear and thermal cracks in some degree.

Most likely, it is the thermal cracks and the crater wear that initiate the fracture. When the crater wear has caused a sufficient loss of material on the rake side of the tool, the cutting edge becomes weakened by the loss of supportive material and becomes more prone to breakage or fracture. A similar sequence of events take place when the thermal cracks grows larger. The notches in the cutting edge weakens it the larger they become and will eventually cause a fracture and further loss of substrate material.

5.4.1. Variation of tool wear

There are considerable variations in the degree of wear between the examined series of tool inserts, it ranges from almost no wear to such a high level of deterioration that the manufacturing were forced to halt in order to replace them prematurely. In series 8 for example, half of the inserts had the lowest degree of wear and only one insert had the second highest amount of wear. Compared to series 4, were nine out of ten inserts had a severe level of wear, the fluctuation of tool wear is significant.

The amount of tool wear is fairly spread out. That is, there is a balance between the number of series with a high level of tool wear and with a low level of tool wear. This can be seen in Figure 4-23 that displays the degree of tool wear in the series of examined tools.

5.4.2. Representability of collected cutting inserts

In series 2 to 10, ten out of 26 inserts mounted on the milling head were examined. Optimally, all 26 inserts should be examined to give the best statistical data. However, a balance between cost, time and data had to be made. Ten inserts were not as good as 26, but it should be enough to give reasonably high certainty of the data.

In series 1, only six inserts were collected. When the data collection started, it was uncertain how much time the examination of the inserts would take and how many data series were to be collected which is why this relatively low number was determined. After the collection and examination of the first series of inserts, it was however clear that there was time enough to examine more inserts and the number of collected inserts were increased to ten.

Six inserts should be enough to give an idea of the degree of tool wear on the inserts during the machining of a series of engine blocks. The greater problem lies in the comparison between the series with six inserts and the other series, which had ten. To solve this the data points in series 1 were scaled up to match the other series. This was done by simply multiplying each data point with $\frac{10}{6}$. Originally, three inserts deemed to have a wear level of 3 in series one. When scaled up, the new number of inserts deemed to have a wear level of 3 became $3 \cdot \frac{10}{6} = 5$.

This way to scale up the data is not ideal since there are so few data points. It is possible that some data points were given an unrepresentative high value, for example, the level 3 wear became very high, and since there were no level 4 wear found it was given the value zero even though it is possible that at least one such insert could have been found if more inserts were examined. However, it is the best way of handling the problem and it gives reasonable good data to work with.

5.4.3. Tool wear and graphite structure

There are no clear correlation between graphite structure and tool wear. Block 3 gave rise to the most amount of tool wear when machined, in this blocks graphite distribution in the surface were type E, D and D. This was the exact same distribution as in block 5, which was the easiest to machine. Block 1 and 2 gave rise to a moderate amount of tool were and in these blocks distribution type A, and in one case D, were found. This suggest that type A is a graphite distribution that produces predictable tool wear when machined. However, there are not enough data to state this with any greater certainty.

5.4.4. Hardness and tool wear

In Table 5-4 the mean hardness of the surface material in the 5 examined blocks are presented compared with the wear ranking of those tools that were used during machining of said material. For easier comparison the hardness of the blocks are ranked from softest (1) to hardest (5).

Table 5-4*: Hardness compared to tool wear. Highest degree of tool wear is 1 and lowest 5. Softest material sample is 1 and hardest 5.*

Material	Tool wear ranking	Ranking of hardness	Hardness Brinell
Block 3	1	3	200.7
Block 4	2	1	197.3
Block 2	3	2	199.7
Block 1	4	4	205.0
Block 5	5	5	211.0

The data indicates that there are a relationship between the hardness of the material and the tool wear. The harder the material is the easier it seems to machine it. Block 5 who has the lowest degree of tool wear is also has the hardest material. Block 1 has the second lowest degree of tool wear and has the second hardest material. On the other end of the scale, block 4 has the second highest degree of wear and the lowest hardness.

The relationships is however not absolute, Block 3 that had the highest degree of wear only has the third softest material. But since Block 3 and 2 has almost identical hardness and block 4 is not far behind it could be said that there is a tendency to lower tool wear when the hardness is greater and vice versa. As discussed in section 5.2.2 Hardness and inclusions, harder material samples has a lower concentration of inclusions and vice versa. It is therefore likely that it is not the hardness of a material itself that makes it easier to machine but rather the absence of Ti(C,N)-inclusions. The correlation between inclusions and tool wear will be further discussed in the section below.

5.4.5. Ti(C,N)-inclusions and tool wear

There is a strong relationship between the degree of tool wear and the concentration of Ti(C,N)-inclusions found in the workpiece material. With no exception, the degree of tool wear increases when the concentration of Ti(C,N)-inclusions increases. In Table 5-5 the tool wear ranking, were place 1 represents the highest degree of wear, and the concentration Ti(C,N)-inclusions are compared.

Table 5-5*: Degree of wear compared to the concentration of inclusions.*

Block	Tool wear ranking	Concentration of Ti(C,N)
3	1	Highest
4	2	Second Highest
2	3	Middle
1	4	Second lowest
5	5	Lowest

The results in this study indicates that it is the concentration of Ti(C,N)-inclusions that more than any other factor is what causes the variation of tool wear. This is in line with what was suspected by the Volvo corporation before this study started and what can be expected according to previous studies [15] [16] [19]. Titanium carbonitride is an extremely hard material, even harder than aluminum oxide that serve as a coating on the cutting edge [17] [25]. Since the Ti(C,N)-inclusions are harder than the coating and the cutting tool material it will subjects the cutting edge to a heavy and continuous abrasive wear that weakens it and makes it more prone to chipping and fracture. The higher the concentration of inclusions are the higher this wear will be.

The polar diagram in Figure 5-2 shows in a schematic way how the machinability of grey cast iron changes when the concentration of Ti(C,N)-

inclusions increases. The abrasiveness will substantially increase and the hardness will slightly decrease, resulting in an overall more difficult material to machine.

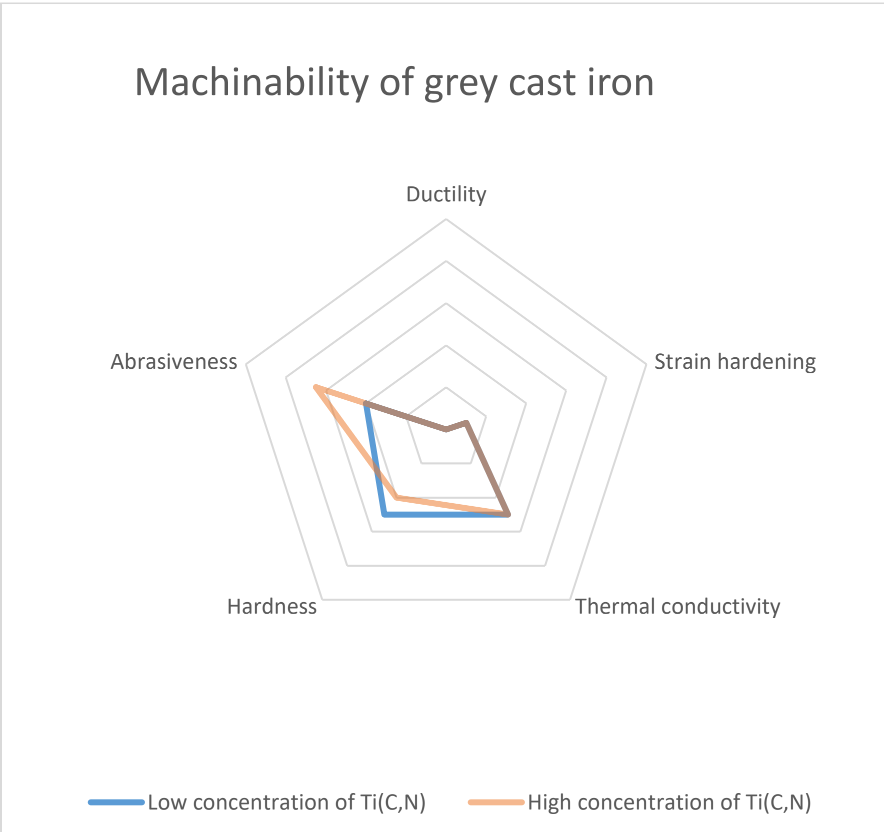

Figure 5-2*: The machinability of grey cast iron with low and high concentration of Ti(C,N)-inclusions.*

6. Conclusion

The results indicates that there is a high, but evenly distributed, variation of tool deterioration found in the inserts used during machining. That is, it is as common for the inserts to have a low degree of wear as it is for them to have a high degree of wear. All levels in the spectrum is represented in the 10 series of examined cutting inserts, from such high degree of deterioration that the machining had to be aborted to such levels that the wear on the inserts were barely visible.

Variations were also found in the grey cast iron that the casted engine blocks were made of. The fluctuation were of different size in the three material factors inclusions, graphite structure, and hardness. Hardness was the material factor that had the least variation between the samples. Most of them had a hardness of 198-202 HB, but some samples had a hardness of up to 211 HB or as low as 187 HB. There was a weak correlation between the graphite structure and the hardness, graphite distribution type A was the softest with an average of 197.7 HB and type E and D the hardest with 205.0 HB and 205.8 respectively. There were also a correlation between hardness and tool wear; generally, harder samples came from series which had lower degree of tool wear. However, this was due to the fact that a low concentration of Ti(C,N)-inclusions made the material harder and hence easier to machine.

Three different types of graphite distributions were found; type A, D, and E. Type A was the most common and E the least common. There are no clear correlation between graphite structure and tool wear. Block 3 gave rise to the most amount of tool wear, in this block the graphite distribution in the three examined areas were of type E, D and D. This exact distribution was also found in block 5 that was the easiest to machine. Block 1 and 2 gave rise to a moderate amount of tool were and in these blocks only distribution type A were found.

The inclusions found in the workpiece material were examined by use of a SEM-XEDS. The results states that these are compounded of manganese sulfides or, less usual, of titanium carbonitrides The concentration of Ti(C,N)-inclusions varied in a high degree between the engine blocks. The highest concentration, found in block 3, was almost double that of the concentration of block 5 which had the lowest concentration. There is a strong relationship between the concentration of Ti(C,N)-inclusions found in a material and the amount of tool wear on those inserts used to machine them. With no exception the engine block became harder to machine the higher the concentration of inclusions were. The Ti(C,N)-inclusions are extremely hard, even harder than the coating of the cutting tools. This hardness subjects the cutting tool to a high and continuous abrasive wear that that weakens the cutting edge and eventually leads to fracture.

In summary, the data states that there are a high variation in the degree of tool wear between manufacturing series as well as in the physical features of the material that is machined by the tools. The data suggest that the variation of tool wear is linked to the concentration of Ti(C,N)-inclusions. However, the amount of data is not enough to draw any clear or certain conclusions.

The findings and conclusions of this report are summarized in the list below:

- Thermal cracks and crater wear are the main wear types acting on the cutting tool. If the crater wear or the thermal cracks becomes sufficiently large they will eventually cause fracture and a substantial amount of material loss in the cutting tool.
- The amount of tool wear differs substantially from one series to another.
- The inclusions were found to be manganese sulfide and titanium carbon nitrides Ti(C,N).
- There is a strong correlation between the concentration Ti(C,N)-inclusions and the degree of tool wear.
- The amount of titanium found in the material correlates with the concentration of Ti(C,N)-inclusions.
- Ti(C,N)-inclusions in this study could be up to 10 µm. They tend to be rectangular and to have sharp edges.
- Trace elements differs significantly in concentration between series.
- There are a substantial variation of the graphite distribution between the samples.
- There is a variation of the hardness of the material, however only marginally.

- There is some variation of hardness between different graphite distribution types.
- Material samples with a low concentration of Ti(C,N)-inclusions are harder than those with low concentration of Ti(C,N)-inclusions
- Harder material tends to be cause less tool wear and softer material tends to cause more tool wear. This is not caused by the hardness itself but rather the correlation between a low concentration of inclusions and high hardness.

7. Further work

Numerous factors affect the material properties of grey iron, in this study the focus has only been on graphite structure, hardness and Ti(C,N)-inclusions. Other factors such as cooling time and aging time should also be analyzed in order to give a certain answer on what causes the variation of tool wear. The tests conducted in this study should also be repeated to give a higher statistical certainty of the results.

How the graphite structure affected the tool wear in this study was not understood. Since this material property have a heavy impact on the machinability, further tests and analyzes should be made to investigate this.

Furthermore, this stud has only investigated the cause of the variation of tool wear and not the solution to it. Naturally, the next step is to look for a way to solve the problem. A reasonable thing to start with is to analyze the cost of premature tool replacement and what savings could be made if the tool replacement interval was to be prolonged.

8. References

[1] J.-E. Ståhl, Metal cutting theories and models, Lund, 2012.

[2] American Foundry Society, "Census of world casting productio," *Modern Casting,* pp. 22-25, December 2019.

[3] A. Diószegi, On microstructure formation and mechanical properties in grey cast iron, Jönköping, 2004.

[4] D. G. R. William D. Callister, Fundamentals of material science and Engineering - An integrated approach, 5th edition, 2016.

[5] Industrial metallurgists, "/www.imetllc.com/training-article/phase-diagram/," [Online]. [Accessed 20 October 2020].

[6] E.-L. Bergquist, Materiallära - Grunderna, Svetsen, 2017.

[7] Svenska gjuteriföreningen, "https://www.gjuterihandboken.se/handboken/3-gjutna-material/32-graajaern," [Online]. [Accessed 08 February 2021].

[8] R. Singh, Applied welding Engineering (Second edition), Elsevier Inc, 2015.

[9] International organization for standradization, ISO 945-1:2008(E), Geneva, 2008.

[10] Totalmateria, "https://www.totalmateria.com/page.aspx?ID=CheckArticle&site=kts&NM=84," August 2002. [Online]. [Accessed 10 January 2021].

[11] J. R. Brown, Fosesco Ferrous Foundrymans handbook, Elsevier Ltd, 2000.

[12] Metal casting institute, "https://metalcastinginstitute.com/iron-types/," [Online]. [Accessed 10 February 2021].

[13] W. D. Callister, Materials science and engineering, 2007.

[14] A. N. R.E. Smallman, Physical Metallurgy and Advanced Materials, 7th Edition, Birmingham, 2007.

[15] S. Sirén, "Processutbildning skärande bearbetning," Skövde, 2019.

[16] A. K. P. G. J. Niclas Ånmark, The Effect of Different Non-Metallic Inclusions on the Machinability of Steels, Stockholm, 2015.

[17] Surface Solutions Incorporated, "Tincoat," [Online]. Available: https://www.tincoat.net/coatings-offered/ticn-titanium-carbo-nitride/. [Accessed 26 02 2021].

[18] Y. S. W. Yan, "Effect of TiN inclusions on the impact toughness of low-carbon microalloyed steels.," 2006.

[19] A. C. A. C. S.B. Singh, "A study of the effect of inclusion content of the machinability and wear characteristics of 0.24% carbon steels," Elsevier B.V., 1997.

[20] J.-E. Ståhl, Metal cutting thories in practice, Lund - Fagersta, 2014.

[21] Sandvik, "https://www.sandvik.coromant.com/en-us/knowledge/materials/pages/wear-on-cutting-edges.aspx," Sandvik. [Online]. [Accessed 20 10 2020].

[22] Hardness testers, "https://www.hardnesstesters.com/test-types/brinell-hardness-testing," [Online]. [Accessed 05 February 2021].

[23] Meghan Tare, Oorvashi Roy Puli, Sarah Oros, Amit Singh, "Drosophila adult eye model to teach Scanning Electron Microscopy in an undergraduate cell biology laboratory," 2009.

[24] Walter Tools, "Walter-tools," [Online]. Available: https://www.walter-tools.com/en-gb/search/pages/default.aspx?m=7220850#/product/XNMF090612-D27%20WKP25S. [Accessed 12 02 2021].

[25] Ceramaret, "Ceramaret," [Online]. Available: https://www.ceramaret.ch/en/technologies/ceramic-materials#:~:text=Aluminum%20oxide%20or%20alumina%20(Al,hardness%20value%20of%20about%202000.. [Accessed 26 02 2021].

[26] N. Ånmark, "Inclusion characteristics and their link to tool wear," Division of Applied Process Metallurgy Department of Materials Science and Engineering School of Industrial Engineering and Management KTH Royal Institute of Technology, Stockholm, 2015.